Ostfalia
Hochschule für angewandte
Wissenschaften

CARBON LOSS IN THE ORGANIC SOIL UNDER AGRICULTURAL USE IN SEVERAL EUROPEAN COUNTRIES

Xiaofeng Li (70456417)

Bachelor’s thesis
January 2018
Bio- and Environmental Engineering
Faculty of Supplied Engineering

ABSTRACT

Ostfalia Hochschule für angewandte Wissenschaften
Ostfalia University of Applied Sciences
Bio- and Environmental Engineering
Faculty of Supplied Engineering

Xiaofeng Li:
Carbon Loss in the Organic Soil under Agricultural Use in Several European Countries

Bachelor's thesis 76 Pages, appendices 13 Pages
January 2018

Global warming occurred in the past without manmade activities, the Earth was warme6d 5 degrees Celsius during the period of 5,000 years from the Little Ice Age. Over the past century, the global temperature rose approximately 1,1 degrees Celsius, which is roughly ten times faster than the ice-age-recovery warming rate. The unusually rapid warming is caused by the extremely increasing amount of greenhouse gases in the atmosphere, which are carbon dioxide, methane, nitrous oxide and fluorinated gases. Energy, industrial processes and product use, agriculture, land use, land-use change and forestry, waste and other are recognised as the greenhouse gases sources according to statistics from the European Commission. The sector of land use, land-use change, and forestry contributes approximately 10 percent to the total greenhouse gas emissions in the European Union member countries. Globally, it accounts for 15 to 20 percent of the total emissions. Vegetation and soil make up the largest terrestrial carbon pool and global carbon pool in terms of carbon exchange with the atmosphere. Therefore, determining the carbon loss from organic soils becomes significant research for global warming.

Carbon in the organic matter is converted to carbon dioxide by microbial decomposition under aerobic conditions, while anaerobic conditions enhance the production of methane. Agricultural cultivation and drainage of lands introduce oxygen into soil pores, which accelerate the production of carbon dioxide, thus increasing the rate of carbon emissions to the atmosphere.

Sites with a variety of land cover types are studied in Denmark, Estonia, Germany, and the Netherlands. Parameters of bulk density and loss of ignition are measured for the calculation of carbon losses. A statistical analysis of agricultural cultivation time, land cover types, decomposition and its influencing factors on carbon loss was conducted. The obtained data shows that a longer cultivation history exhibits higher levels of carbon loss for a certain land cover type. In addition, soils that are high in carbon stock show high levels of carbon loss. The value of carbon loss through the intensively managed grassland is the highest, while carbon loss through the arable land is the second highest. Appropriate soil conditions beneficial for microbial decomposition promote an increasing level of carbon loss.

Key words: global warming, soil, decomposition, drainage, cultivation, carbon loss

TABLE OF CONTENTS

1 INTRODUCTION 8
  1.1 An overview of global climate change since industrial era 8
  1.2 The carbon cycle involving carbon pools and carbon fluxes 9
  1.3 Land cover/use in Europe 11
  1.4 Organic soils and microbial decomposition 12
  1.5 The structure and aims of the work 13
2 MATERIALS AND METHODS 14
  2.1 Site description 14
  2.2 Soil cores sampling and storage 16
  2.3 Data collection in the laboratory 16
    2.3.1 Determination of bulk density 17
    2.3.2 Determination of ash content and the loss of ignition 19
  2.4 Analysis with R language programme 22
    2.4.1 Determination of the carbon loss 22
    2.4.2 Functions developed for statistical analysis 24
3 RESULTS 33
  3.1 Results of bulk density and Loi obtained from the laboratory 33
    3.1.1 Denmark 34
    3.1.2 Estonia 38
    3.1.3 Germany 43
    3.1.4 The Netherlands 45
  3.2 Carbon loss and statistical analysis 49
    3.2.1 Carbon loss in response to land use types 49
    3.2.2 Carbon loss in response to land use types and cultivation time 51
    3.2.3 Carbon loss in response to factors influencing the decomposition rate 53
4 DISCUSSION 55
  4.1 Discussion on the bulk density and Loi 55
  4.2 Discussion on land use types influencing the carbon loss 56
  4.3 Discussion on factors influencing the decomposition rate of organic matters 56
  4.4 Recommendations 58
5 CONCLUSIONS 61
REFERENCES 62
APPENDICES 64
  Appendix 1. Table of compiled data for statistical plots 64

Appendix 2. The geographical locations and the description of sites 65
Appendix 3. Human influence on the GHGs 66
Appendix 4. Trends, estimation, and targets of GHGs in the EU, 1990-2050 67
Appendix 5. A comparison of GWP 68
Appendix 6. The global greenhouse gas emission 69
Appendix 7. The greenhouse gas emission by source sector in EU 70
Appendix 8. Data comparison among EPA, EDGAR, and FAO on GHGs emission from agriculture sector 71
Appendix 9. GHGs emission from the agriculture sector in different regions in comparison to several data sources 72
Appendix 10. The GHGs emission in EU-28, 2012 (Eurostat. 2016) 73
Appendix 11. Table of carbon loss and its influencing factors at sites 74
Appendix 12. Tables of pristine carbon and carbon loss at sites 75
Appendix 13. A comparison of carbon loss and pristine carbon at sites 76

LIST OF PICTURES

PICTURE 1 A soil core sample (B. Tiemeyer. 2017) 16
PICTURE 2 Cutting soil core in the laboratory 18
PICTURE 3 Soil core segments in aluminum trays 19
PICTURE 4 Grinding and screening samples 20
PICTURE 5 Samples in ceramic dishes before being calcined in muffle furnace 21

LIST OF FIGURES

FIGURE 1 A simplified diagram of the carbon cycle. (Source: IPCC Report. 2001) 10
FIGURE 2 Statistics of land cover in Europe in 2015. (Source: Eurostat) 12
FIGURE 3 Map markers of the studied sites in Europe 14
FIGURE 4 Creating a bar plot of cultivation time associated with carbon loss 27
FIGURE 5 Creating a bar plot of land use associated with carbon loss 29
FIGURE 6 Creating a bar plot 30
FIGURE 7 Layout of the plot 32
FIGURE 8 Generation of a linear regression model in R 32
FIGURE 9 Adding the error bar on the plot 32
FIGURE 10 Bulk density and Loi at the first site in Denmark (N 56°27', E 9°40') 35
FIGURE 11 Bulk density and Loi at the second site in Denmark (N 56°27', E 9°40') 36
FIGURE 12 Bulk density and Loi at the third site in Denmark (N 56°29', E 9°51') 37
FIGURE 13 Bulk density and Loi at the fourth site in Denmark (N 56°29', E 9°51') 38
FIGURE 14 Bulk density and Loi at the first site in Estonia (N 58°30', E 27°0') 39
FIGURE 15 Bulk density and Loi at the second site in Estonia (N 58°15', E 26°9') 40
FIGURE 16 Bulk density and Loi at the third site in Estonia (N 58°15', E 26°9') 41
FIGURE 17 Bulk density and Loi at the fourth site in Estonia (N 58°13', E 26°17') 42
FIGURE 18 Bulk density and Loi at the fifth site in Estonia (N 58°13', E 26°17') 43
FIGURE 19 Bulk density and Loi at the first site in Germany (N 48°30', E 10°15') 44
FIGURE 20 Bulk density and Loi at the second site in Germany (N 48°30', E 10°18') 45
FIGURE 21 Bulk density and Loi at the first site in The Netherlands (N 51°56', E 4°43') 46
FIGURE 22 Bulk density and Loi at the second site in The Netherlands (N 51°56', E 4°43') 47

FIGURE 23 Bulk density and Loi at the third site in The Netherlands (N 52°8', E 4°50') 48
FIGURE 24 Bulk density and Loi at the fourth site in The Netherlands (N 52°8', E 4°50') 49
FIGURE 25 Carbon loss associated with land use types 50
FIGURE 26 Carbon loss associated with lands covered by grass and crops 51
FIGURE 27 Carbon loss associated with cultivation time and land use types 52
FIGURE 28 Factors influencing decomposing rate in organic soil I 53
FIGURE 29 Factors influencing decomposition rate in organic soil II 54

LIST OF TABLES

TABLE 1 Reading files in R environment 25

ABBREVIATIONS AND TERMS

CH_4	Methane
C.kg_m^2_sem	The standard error of the median of carbon stock
C.kg_m^2	The carbon stock unit kilo gram per square meter
CLoss.kg_m^2_sem	The standard error of the median of carbon loss
CLoss.kg_m^2	The carbon loss in unit kilo gram per square meter
CO_2	Carbon dioxide
CO_2eq	The gas emission unit in CO_2 equivalent
CPristine.kg_m^2_sem	The standard error of the median of pristine carbon
CPristine.kg_m^2	The pristine carbon in unit kilo gram per square meter
DK	Denmark
DO	Germany
EDGAR	Emission Database for Global Atmospheric Research
EE	Estonia
EEA	European Environment Agency
EIT	Economies in Transition
EPA	United States Environmental Protection Agency
FAO	Food and Agriculture Organization of the United Nations
GHGs	Greenhouse gases
IPCC	Intergovernmental Panel on Climate Change
LAM	Latin America and the Caribbean
LULUCF	Land Use, Land-use Change, and Forestry
MAF	Middle East and Africa
N_2O	Nitrous oxide
NLS	the Netherlands
OECD-1990	Organisation for Economic Co-operate and Development
Pg	Petagrams = 10^{15} g, equals to Gigaton (Gt)
S.m_sem	The standard error of the median of subsidence
S.m	The subsidence in unit meter
Sp.m_sem	The standard error of the median of primary subsidence
Sp.m	The primary subsidence in unit meter
Ss.m_sem	The standard error of the median of secondary subsidence
Ss.m	The secondary subsidence in unit meter

1 INTRODUCTION

1.1 An overview of global climate change since industrial era

Approximately 71 percent of the solar energy is absorbed by the Earth system, whereas 23 percent of the incoming sunlight is absorbed by the water vapour, dust and the ozone in the atmosphere. Another 48 percent of it passes through the atmosphere and is absorbed by the surface of the ocean and the Earth's land. About 29 percent of the solar heat is reflected back to space by clouds, atmospheric particles, polar ice, and snow (R. Lindsey. 2009). The Earth's energy balance had been kept in a stable state under the function of a natural mechanism. Ever since industrial revolution between the 18th and 19th century, fossil fuel powered plants and transportation produce a large amount of carbon dioxide, methane, nitrous oxide and fluorinated gases (Hydrofluorocarbons (HFCs), perfluorocarbons (PFCs), sulphur hexafluoride (SF_6) and nitrogen trifluoride (NF_3)), which are known as greenhouse gases. The greenhouse gases prevent reflection of the solar heat from Earth back to space and trap it in the atmosphere instead. This process is called greenhouse effect. With the continuously increasing amount of greenhouse gases produced, the global temperature has risen 0,7 Celsius degrees over the last century, which is approximately 10 times faster than the average rising rate in past ice ages (NASA. 2007), this phenomenon is called global warming. Global warming could not only lead to polar ice melting but also displace cities and tropical islands of planet Earth's maps.

According to the European Environment Agency (EEA), greenhouse gases are produced from six sectors, which are: energy, industrial processes and product use, agriculture, LULUCF (land use, land-use change, and forestry), waste and other. The data of greenhouse gas emission from each sector worldwide and within the European Union can be found in Appendix 5 and Appendix 6. As shown in Appendix 2, according to the Climate Change 2001 report by the Intergovernmental Panel on Climate Change (IPCC), the concentrations of greenhouse gases in the atmosphere including carbon dioxide (CO_2), methane (CH_4) and nitrous oxide (N_2O) are increasing during the industrial Era, from year 1800 to year 2000. The concentration of CO_2 increased from around 280 ppm to over 360ppm, the concentration of methane increased from 750 ppb to nearly 1750 ppb and the concentration of nitrous dioxide increased from around 270 ppb to over 310 ppb. (J.T.Houghton, Y.Ding, et al. 2001)

On a global scale, the greenhouse gas emission is increasing over time (IPCC. 2014). However, the GHGs emission in Europe is generally decreasing by 2015 according to observed data, since employing the mix of fossil fuels and renewable energies, in addition to a reduction of energy demand for heating houses due to a milder winter period in Europe during the observing period. In 2013, Europe fulfilled ahead of the 2020 target that achieving a reduction of GHGs emission by a 20 percent (EEA). The aim for 2030 is to implement a CO2 emissions reduction by 40 percent. In order to achieve the GHGs emission targets by 2030 and 2050, research on factors that influence GHGs emission from each economic sector is significant, wherein, the GHGs emission from sector LULUCF is quite challenging.

1.2 The carbon cycle involving carbon pools and carbon fluxes

The carbon cycle brings prime interests to scientists due to two main reasons, on the one hand, compounds of carbon dioxide and methane are one of the greenhouse gases causing global warming, the level of atmospheric carbon dioxide is observed to keep rising; on the other hand, carbon element is vital for building all living organisms and forming necessary compounds (D. Schimel, I.G.Enting, et al. 2000). Carbon is present not only in the atmosphere (mainly in the form of carbon dioxide (CO_2) and the other less plentiful but highly significant gas concerning changing global climate such as methane (CH_4)) but also in oceans and land ecosystems. (NOAA). Carbon pools, which are also known as carbon stocks, carbon sinks and carbon reservoirs, refer to components in the Earth system. A large amount of carbon is stored in the atmosphere, ocean, crust, vegetation, and soil. Carbon pools function both, as sources for inputting carbon into the atmosphere and taking out carbon from the atmosphere.

Studying carbon pools can help scientists understand the carbon cycle and the reason for global warming, as well as the future trend of atmospheric CO_2. Carbon pools are divided into four categories according to the extent of relevance to the carbon cycle; the Earth's crust, oceans, atmosphere and terrestrial ecosystems. At a global scale, sedimentary rocks make up for the biggest carbon pool on Earth, which store 100,000,000 Pg carbon mainly in the form of carbonate. The Earth's crust stores 4,000 Pg hydrocarbons, known as fossil fuels that formed from ancient living organisms over a period of millions of years. 38,000 Pg carbon in the form of dissolved inorganic carbon is stored in the great depths of oceans.

About 1,000 Pg carbon is stored at the ocean surface, where carbon exchange with atmospheric carbon via dissolved CO_2, photosynthesis, respiration and decomposition takes place. The atmosphere stores approximately 750 Pg carbon, which mainly exists in the form of carbon dioxide and a much less amount of methane (CH_4). Plants and soils contain a larger amount of carbon comparing to animals and microorganisms in terrestrial ecosystems, whereas plants store approximately 560 Pg carbon and soils store 1500 Pg carbon. The carbon in soils is primarily in the form of organic carbon originated from dead organic matters. The access of oxygen to soil pores promotes an aerobic decomposition of organic matters by microbes, which produces CO_2. (UNH. 2009).

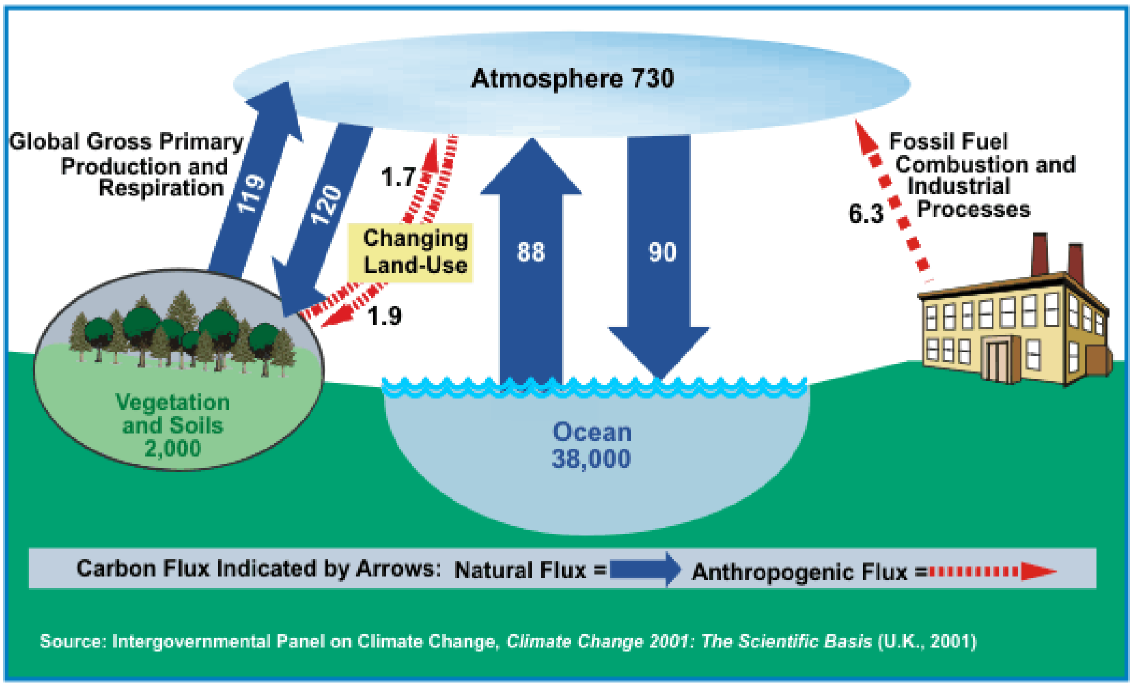
Atmosphere 730
Global Gross Primary Production and Respiration
119
120
1.7
Changing Land-Use
1.9
88
90
Fossil Fuel Combustion and Industrial Processes
6.3
Vegetation and Soils 2,000
Ocean 38,000
Carbon Flux Indicated by Arrows: Natural Flux = Anthropogenic Flux =

Source: Intergovernmental Panel on Climate Change, *Climate Change 2001: The Scientific Basis* (U.K., 2001)

FIGURE 1 A simplified diagram of the carbon cycle. (Source: IPCC Report. 2001)

The movement of carbon from one pool to another is called a carbon flux. Carbon fluxes enhance the carbon exchange among carbon pools, both carbon fluxes and carbon pools comprise the global carbon cycle (UNH. 2008). As shown in Figure above, the numbers inside the arrows refer to carbon fluxes measured in petagrams (Pg) of carbon per year. The numbers outside the arrows refer to the carbon pool sizes in petagrams (Pg) of carbon. Carbon from the atmosphere is transferred to vegetation via photosynthesis with the presence of water and sunlight, meanwhile, carbon is released back to the atmosphere via respiration, fire, harvesting, as well as decomposition and decay in organic matter over years. The same carbon cycle is also linked to oceans. The exceed inputs of carbon dioxide produced during the process of fossil fuel combustion to the atmosphere and deforestation enlarges the atmospheric carbon size, which destroys the previous carbon balance in all carbon pools. (UNH. 2008)

Soils store the largest amount of carbon at a global scale in terms of the ability for carbon exchange with the atmosphere. As the statement above, soils store 2000 Pg carbon, the atmosphere stores 750 Pg carbon, oceans stores 38,000 Pg carbon while approximately 1000 Pg carbon at the ocean surface exchanging carbon with atmosphere. Thereby soils have the greatest capability to provide and support carbon cycle and are of special interest to research regarding the reasons for carbon loss from soil.

1.3 Land cover/use in Europe

The following paragraph is a brief overview of the land cover in Europe. Land cover refers to the biophysical coverage of land. Land cover can be grass, crops, shrubs, water, broad-leaved forest, or a built-up area. There is an intertwined concept of land cover called land use, which is defined as the application of the land in terms of socio-economic benefits, for instance, agriculture, forestry, industrial or service use, residential use (Eurostat. 2016).

According to the latest Land Use and Coverage Area frame Survey (LUCAS) by EUROSTAT in 2015, the primary sector of land cover in Europe is woodland, which accounts for 37,8 percent of the total surface area. The secondary sector is cropland, accounting for 22,2 percent of the entire European land cover. The tertiary sector is grassland, accounting for approximately one-quarter of the land cover at 20,7 percent of the land. The other land cover such as shrub land, accounting for 7,1 percent of the whole land cover. Therefore, grassland and arable cropland have much of the same proportion of the total land areas in Europe.

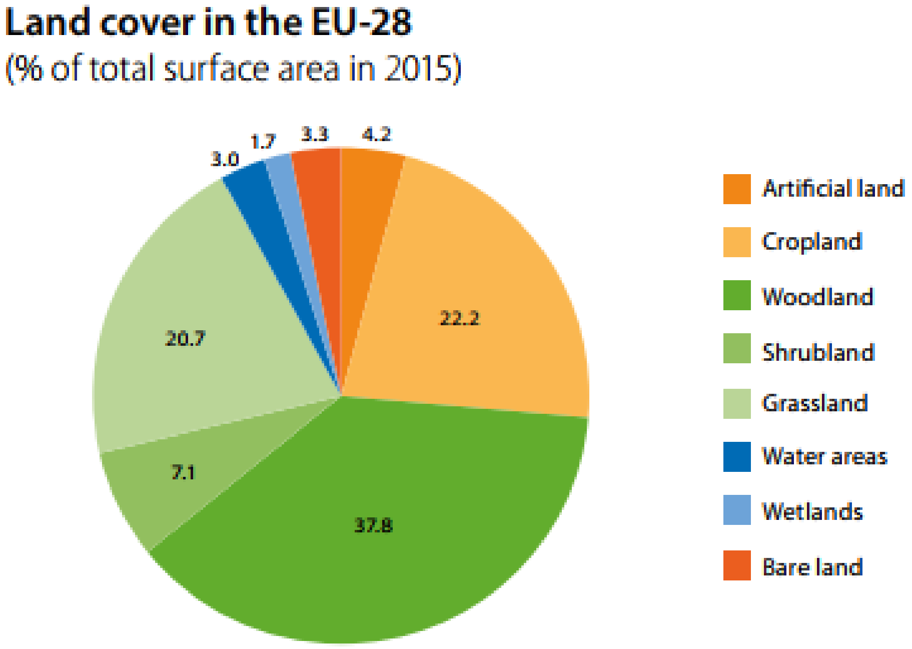

FIGURE 2 Statistics of land cover in Europe in 2015. (Source: Eurostat)

1.4 Organic soils and microbial decomposition

As shown in Appendix 5 and Appendix 6, in 1990 and 2015 (updated statistics would be available in February 2018), agriculture contributed 10 percent to the total GHGs emission in the European Union. Agriculture and forestry together comprise 24 percent of GHGs emission globally (IPCC. 2014; EEA. 2017). The agricultural sector comprises the greatest contributor to global anthropogenic non-CO_2 GHGs emission source, which accounts for 56 percent of the whole emission in 2005 (U.S. EPA, 2011). According to IPCC reporting guidelines, agricultural sector covers emissions from enteric fermentation, rice cultivation, agricultural soils, and manure management systems. Agricultural soils are the largest GHGs emission source global based on the database of EPA 2006 and EPA 2011 (see Appendix 7), and is the dominant GHGs emission source in the European Union accounting for over 51 percent in the agricultural sector (see Appendix 9). GHGs emission generated from agricultural soil comprises 5,3 percent of the total emission in the European Union (Eurostat. 2016). Thereby, observing GHGs emission from soil pool is essential to study the agricultural influence on global warming. Peat soils store over 600 Pg carbon that constitutes 30 percent of the total carbon in soil pool (J.P.Krüger et al., 2015; Yu et al., 2011; Jungkunst et al., 2012). From an objective perspective, studying peat is significant to investigate GHGs emission from soil.

In the 20th century, more than half amount of peat lands in Europe were transformed to agriculture and forestry (J.P.Krüger et al., 2015; Byrne et al., 2004). Anaerobic environment limits the microbial break down of organic materials. The degradation of organic matters by microbes under the anaerobic environment is a reduction process, which more possibly enhances the production of CH_4 with a small portion of CO_2. Agricultural cultivation enhances the aerobic environment by drainage; the oxygen is introduced into the soil pores due to enhanced diffusion in the air filled pores and enhanced oxygen availability in regularly ploughed top soils. With the presence of air, organic materials in the soil could be further decomposed during an aerobic oxidation process, where two-thirds carbon from organic matters is converted into CO_2 and emitted to the atmosphere, the other one-third carbon is combined with nitrogen in cells.

1.5 The structure and aims of the work

Concepts of global climate change, the carbon cycle involving carbon pools and carbon fluxes, the land cover in Europe, the significance of organic soils and microbial decomposition are introduced in the INTRODUCTION chapter. Site description and sampling, likewise, the preparation of samples and data collection, as well as statistical analysis with R language are provided in the chapter of MATERIALS AND METHODS. Results obtained from the laboratory are managed with R language and presented in the RESULTS chapter. The analysis of the obtained results, subjective and objective factors influencing the results and error propagations are discussed in the DISCUSSION chapter. The main findings regarding the effects of agricultural cultivation time, land cover types and microbial activities on carbon loss are concluded and the hypothesis of this work is verified, as shown in the chapter of CONCLUSIONS.

The overarching goal is to calculate the carbon loss from organic soil and carry out a statistical analysis of the influence of agricultural cultivation time on the carbon loss in response to certain land cover types. The other goal is to illustrate the hypothesis for this work, which is: i) agricultural cultivation and drainage enhance the release of carbon dioxide from soils to the atmosphere during the process of decay so as to contribute to global warming; ii) a longer cultivation time releases a larger amount of carbon loss from soil to atmosphere; iii) arable lands have a larger amount of carbon loss than grasslands.

2 MATERIALS AND METHODS

The parameters of bulk density (ρ_b), loss of ignition (loi) and ash content are measured by employing a laboratory methodology, while R programming method is used for the calculation of the carbon loss, the carbon stock per depth and the statistical analysis of carbon loss associated with the agricultural cultivation time, land cover types, as well as variables affecting microbial activities.

2.1 Site description

Soil core samples were taken from different sites in Denmark, Estonia, Germany, and the Netherlands in 2015 (A. Piayda. 2017). Wherein two sites in Germany, four sites in Denmark, four sites in The Netherlands, and five sites in Estonia were selected (see FIGURE 3). Four soil cores were taken from each site. The sampling was carried out from the surface of the soil down to 1m depth with driving hammer corer.

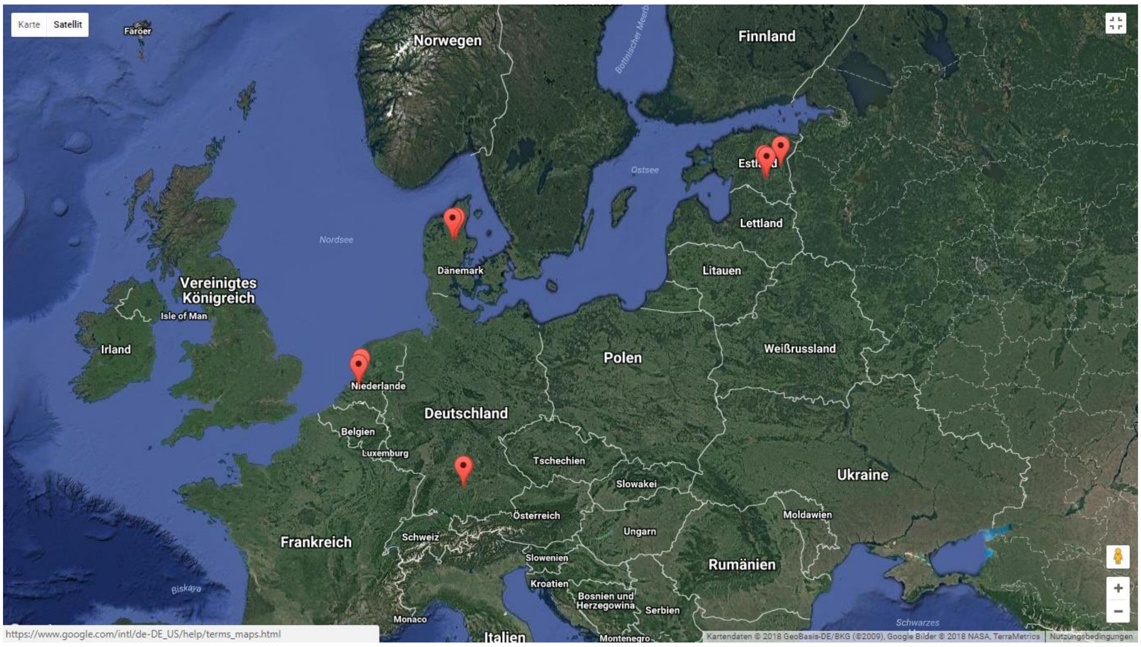
Karte
Satellit
Färöer
Norwegen
Finnland
Bottnischer Meerbusen
Ostsee
Estland
Lettland
Nordsee
Dänemark
Litauen
Vereinigtes Königreich
Isle of Man
Irland
Niederlande
Polen
Weißrussland
Deutschland
Belgien
Luxemburg
Tschechien
Slowakei
Ukraine
Österreich
Moldawien
Ungarn
Frankreich
Schweiz
Slowenien
Rumänien
Kroatien
Bosnien und Herzegowina
Serbien
Biskaya
Monaco
Italien
Montenegro
Schwarzes
https://www.google.com/intl/de-DE_US/help/terms_maps.html
Kartendaten © 2018 GeoBasis-DE/BKG (©2009), Google Bilder © 2018 NASA, TerraMetrics
Nutzungsbedingungen

FIGURE 3 Map markers of the studied sites in Europe

Two sites among all studied areas are located in near Günzburg, Bayern, and southern Germany. The geographical locations of the two sites are rather close (6km apart). The annual temperature is 8,3 Celsius degrees and the average precipitation is 775 mm per year in this area. Günzburg has an altitude of 465 m above the sea level, the climate is temperate oceanic climate (climate-data.org). Site one (N 48°30', E10°15') is an intensively managed grassland, which has been cultivated between 50 and 100 years. Drainage activities began 100 years ago, drainage is only fulfilled by ditches at this site. Site two (N 48°30', E10°18') is located at the south-western of site one, it has been cultivated for more than 100 years and is currently used as a pasture. The drainage history started 100 years ago and the drainage type is the same as site one (A. Piayda. 2017).

In Denmark, soil samples were taken from four sites in Tjele and Randers, on the Jutland peninsula, northern Denmark. Tjele has an altitude of 46 m, which is located at N 56°27' and E 9°40' geographically. The altitude of Randers is 21 m, it belongs to temperate oceanic climate zone, which has an annual average temperature of 7,5 Celsius degrees and its annual mean precipitation is 646 mm (The world bank. 2014). The two sites in Tjele are currently used with paludiculture crops on peat lands, while the other two sites in Randers are used as extensively managed grass lands. All of the four sites have been cultivated for more than 100 years, the drainage activities started 100 years ago and the drainage type is only with ditches.

Soil cores samples from five sites in Estonia were taken. Site one is located at N 58°30' and E 27°0' geographically near Tartu, which is around 15 km apart from the Lake Peipus and about 40 km distanced from Tartu city in eastern Estonia. The annual mean precipitation in Tartu is 599 mm and the average temperature is 5,0 Celsius degrees throughout the whole year. The climate is warm-summer humid continental climate. Tartu has an altitude of 58 m above the sea level. The current use of this land is active peat extraction, the cultivation and drainage history are unknown. The other two sites are located at N 58°15' and E 26°9' geographically in Tartu County (Tartu maakond), south Estonia. The studied areas are around 600 m away from the east side of Lake Võrtsjärv. One of the two sites (Latitude: 58.5, Longitude: 27.0) is covered with grass, which has been intensively managed and cultivated for 55 years. The other site (Latitude: 58.2, Longitude: 26.2) is covered with wheat and cultivated for 55 years until now as well. The drainage type in both sites is only with ditches. The other two sites are located at N 58°13' and E 26°17' in Tartu County as well. The cultivation time of the two sites has been 44 years so far, the drainage type is the same as the other sites in Estonia which is only with ditches. Samples from the site (Latitude: 58.2, Longitude: 26.3) were taken from an intensively managed grassland, while samples from the site (Latitude: 58.2, Longitude: 26.3) were covered with barley. All studied areas are between Lake Võrtsjärv and Lake Peipus.

The studied areas in The Netherlands are located on the west coast in Stolwijk, South Holland. The average temperature in this town is 9,5 Celsius degrees throughout the year, the annual mean precipitation is 799 mm, it belongs to temperate oceanic climate zone (climate-data. org). Two of the four sites are located at N 51°56' and E 4°43', while the other two sites have a geo-location at N 52°8' and E 4°50'. The current land use of all studied areas is intensively managed grasslands, which have been cultivated for more than 50 years but less than 100 years. The drainage types at the site (Latitude: 52.0, Longitude: 4.7) and site (Latitude: 52.1, Longitude: 4.8) are with ditches and underground pipes. Drainage activities started 100 years ago at the site (Latitude: 51.9, Longitude: 4.7), which with only ditches. The site (Latitude: 52.1, Longitude: 4.8) has been drained for more than 50 years by ditches. (A. Piayda. 2017)

2.2 Soil cores sampling and storage

The soil core samples were taken with a driving hammer corer, four replicated cores were taken at each site. In the laboratory, soil core samples were stored by category in the cooling room at 6 Celsius degrees for further analysis.

PICTURE 1 A soil core sample (B. Tiemeyer. 2017)

2.3 Data collection in the laboratory

As mentioned above, four soil cores were taken at each site. Thereby, the laboratory experiment is in four replicates. The first analyzing round started with one of the quadruplicated soil cores from the first site in each country, the second analyzing round started with the second quadruplicated soil cores from the second site in each country. Eventually, all soil cores from countries of Denmark, Estonia, Germany, and the Netherlands were analyzed by following the same procedure.

The preparation of samples and measurements of parameters of ash content, bulk density and the loss of ignition are carried out in the laboratory. The materials and equipment used for developing this method, as well as the laboratory procedures are elaborated in this section.

2.3.1 Determination of bulk density

Materials and equipment:

- Soil cores
- Soil core cutting device
- Knife
- Rule
- Flat iron sheet
- White plastic spacer block
- Triangular Spatula
- Aluminum trays
- Label sheets
- Stainless steel mobile cart
- Electronic balance scale

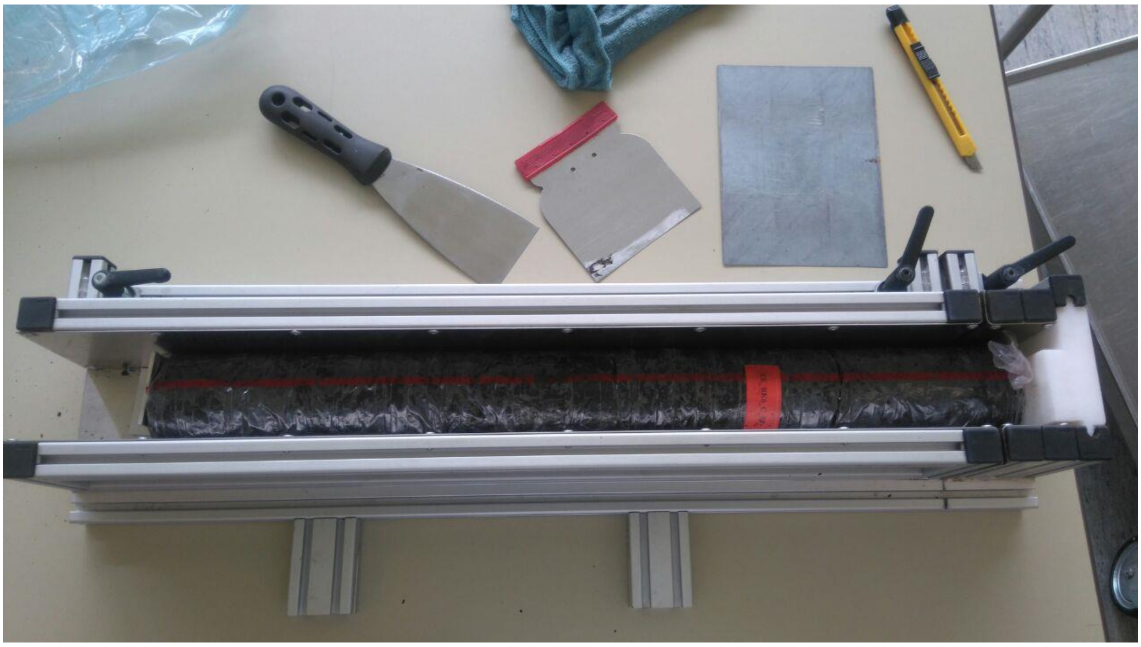

PICTURE 2 Cutting soil core in the laboratory

The target soil cores stored in the cooling storage room at a temperature of 6 degrees Celsius are transported to the soil preparation lab with a mobile cart. Each soil core with a total length of 100 cm is cut into two segments in order for easy transportation to the laboratory. The two cut partial soil cores have different lengths, the longer one always represents the upper part of the original soil core. The orientation of the original soil core is determined by reading the labels of each part of the soil core in the correct direction. Once the topsoil and orientation of the target soil core are determined, the soil core is ready for cutting. The cutting segment is adjusted to 3 cm on the soil core cutting device. The procedures of cutting soil cores are as follows:

The materials and equipment listed above are prepared and ready to be used before transporting target soil cores from the cooling storage room to the laboratory (picture 1). Aluminum trays are labeled and put in order. The right side of the soil core cutting device is blocked with the white plastic spacer block, the upper part of the soil core is placed in the slot and pushed forward naturally until it reaches the spacer block. Fixing the left position of the soil core, placing the knife at the 3 cm position from the right ending side, which has been already set up, using the knife to cut so that a 3 cm of soil core segment can be obtained. The 3 cm soil core segment is placed in the aluminum tray that has been labeled. The outside plastic wrapped plastic film is removed, the soil core segment is broken into smaller pieces.

PICTURE 3 Soil core segments in aluminum trays

Once the whole soil core is cut by following this procedure as seen in picture 2, all soil samples in aluminum trays are stored for 24 hours in the drying oven at a temperature of 80 degrees Celsius. The length of the last segment is noted down if it is not 3 cm.

After drying for 24 hours, the total mass of the dried soil samples and aluminum tray, as well as the mass of the empty aluminum tray were weighed. The mass difference between the two values is determined as the dry mass of the soil sample. Therefore, bulk density (g/cm^3) can be determined by the obtained dry mass and the given volume (radius=2,5cm), as shown in the equation (1) below.

$$Bulk\ density = \frac{mass_{dry\ soil\ and\ aluminum\ tray} - mass_{aluminum\ tray}}{\pi r^2 * 3\ cm} \tag{1}$$

2.3.2 Determination of ash content and the loss of ignition

Materials and equipment:

- Dry soil samples
- Stainless steel wire mesh sieves and screen sets with a 2 mm aperture
- Grinding bowls and rods
- Noise-proof headphones

- Dust-proof masks
- Goggles
- Vacuum dust collector
- Electronic balance scale
- Stainless steel mobile cart
- Desiccators
- Aluminum foil
- Crucible tongs
- Drying oven
- Muffle furnace
- Ceramic dishes and inlays
- Steel stand - For placing ceramic dishes
- Precise electronic balance scale

The dried soil samples are ground by using the grinding bowl and rod. A maximum 2 mm of the particles' diameter is required. The ground samples are stored in the drying oven for another 24 hours. Picture 4 below shows the procedure of grinding samples and screening.

PICTURE 4 Grinding and screening samples

The procedure for determining ash content and the loss of ignition is as follows:

- Ground samples were transported from the drying oven to desiccators to avoid moisture in the atmosphere
- Ceramic dishes were numbered and placed in order
- The masses of the ceramic dishes and inlays were measured and recorded
- About 1 mg samples were taken and put into the inlay, the actual mass of the samples was recorded
- The ceramic dishes were put on the steel stand one by one
- The rest samples in the aluminum trays were put back to the drying oven at 80 ℃.
- The steel stand with samples was put in the muffle furnace at temperature 550 ℃ for 5 hours
- The steel stand with the ash residue was transported from the muffle furnace into the drying oven under 100 ℃ for 2 hours, so as to make sure that the samples can be cooled down without the appearance of moisture
- The ash residue was transported by using stainless steel tongs from the drying oven to desiccators for another 2 hours
- The total mass of the ceramic dish, inlay and ash residue for each sample was measured

PICTURE 5 Samples in ceramic dishes before being calcined in muffle furnace

The ash content is determined by the following equation:

$$\text{Ash content} = \frac{mass_{ceramic\ dish,inlay,ash\ residue} - mass_{ceramic\ dish\ and\ inlay}}{mass_{ceramic\ dish,inlay,sample}} * 100\% \qquad (2)$$

The loss of ignition is determined by the following equation:

$$\text{Loi} = 1 - \text{ash content} \qquad (3)$$

The ash residue in ceramic dishes is discarded, samples in the drying oven that have been analyzed are collected and stored for further utilization.

2.4 Analysis with R language programme

R is a programming language and software environment written by Robert Gentleman and Ross Ihaka, the first letter of the first names of the two authors is used to name this programming language “R”. Currently, R is being developed by the R Core Team. R is used for the statistical analysis and reporting, which are presented in graphs and tables. (tutorial point). The R version 3.4.1 “Single Candle” is employed in this work, the working platform is x86_64-w64-mingw32/x64 (64-bit). (The R Foundation. 2017)

Functions managing obtained data from the laboratory are developed, including reading and writing files, finding median values of different parameters, computing standard error of the median, plotting graphs, finding the reference depth of each analyzed soil core, the calculation of carbon stock, carbon loss and subsidence, as well as statistical analysis, such as the comparison of carbon loss for different cultivation history, the comparison of carbon loss from a variety of land use types and a comprehensive analysis of the two figures.

2.4.1 Determination of the carbon loss

The ratio of carbon and ash content is assumed as a fixed value per depth during the accumulation of organic soils. The ash content is assumed to be constant at all depth before drainage. In addition, drainage does not have an impact on the ash content in the subsoil. The ash content in subsoil is used as a reference data. The carbon loss is determined by the bulk density and subsidence.

The primary subsidence refers to the shrinkage of the layer of organic soils due to physically loss of pore water, it is calculated by the following equations:

$$S_p = PT_{pre\_i} - PT_i \tag{4}$$

$$PT_{pre\_i} = \frac{BD_i}{BD_r} * PT_i \tag{5}$$

$$BD_{o\_i} = \frac{(mass_{sample\_i} - mass_{ash_i})\ g}{\pi * (2{,}5\ cm)^2 * 3\ cm} \tag{6}$$

$$BD_{o\_r} = \frac{(mass_{sample\_r} - mass_{ash\_r})\ g}{\pi * (2{,}5\ cm)^2 * 3\ cm} \tag{7}$$

Where,
Sp refers to the primary subsidence (m)
PT_{pre_i} refers to the pre-thickness of the i layer (m)
PT_i refers to the thickness of the i layer at the moment of sampling (m)
BD_{o_i} refers to the mass of organic matters divided by the volume of the layer i (g/cm^3)
BD_{o_r} refers to the mass of organic matters divided by the volume of the reference layer (g/cm^3)
$mass_{sample\_i}$ refers to the mass of the sample in the ceramic dish of layer i (g)
$mass_{ash_i}$ refers to the mass of the ash residue remained in the ceramic dish (g)
$mass_{sample\_r}$ refers to the mass of the sample in the ceramic dish of the reference layer (g)
$mass_{ash\_r}$ refers to the mass of the ash residue remained in the ceramic dish of the reference layer (g)

The secondary subsidence is caused by the oxidative loss of organic matter, it is defined by the following equations:

$$ST_{pre\_i} = ST_i * \frac{Ash\ content_i}{Ash\ content_r} \tag{8}$$

$$S_s = ST_{pre\_i} - ST_i \tag{9}$$

$$C_{loss} = S_s * \frac{C_{stock\_r}}{ST_r} \tag{10}$$

Where,

Ss refers to the secondary subsidence (m)

ST_{pre_i} refers to the pre-drainage thickness of layer i (m)

ST_i refers to the thickness of layer i (m)

$Ash\ content_i$ refers to the ash content in layer i

$Ash\ content_r$ refers to the ash content in the reference layer

C_{loss} refers to the carbon loss per depth (kg/m^2)

C_{stock_r} refers to the carbon stock per depth (kg/m^2)

ST_r refers to the thickness of the reference layer (m)

2.4.2 Functions developed for statistical analysis

Compiling file

First of all, it is necessary to compile the available and demanded files that separately contain columns of land use types, time since cultivation, carbon loss and the standard error of the median of carbon loss. Afterwards, graphs can be plotted based on the compiled file. The steps of compiling several files by R are the following:

Clearing the workspace by using the function ***rm** (list=ls())*, therefore, the automatically loading objects can be prevented and an entirely clean and empty working environment for R is provided. Setting up the working directory for the entire R operations to carry out, such as data input and output. Function ***setwd ("O:/Rscript")*** can be used to achieve this goal.

It is necessary for R to read data from interested files in the current working directory so that R can access and operate it. The files can be in a variety of formats, such as csv, xlsx, txt, and so forth. Reading the first csv file containing data of carbon loss and the standard error of the median by using function **read.csv(),** a data frame will be created in the R environment. Assigning a name to the data frame, for instance, *carb_subs <- **read.csv(**file = "O:/Rscript/data/output/results_carbon_subsidence.csv",header = T, sep = ","**)***.

read.table() can be used to read txt files. Reading the txt file containing contents of land use types represented by keys and assigning the name “merged_results” to it in R: *merged_results <- **read.table(**"O:/Rscript/data/input/merged_results.txt",header = TRUE, sep = ",", stringsAsFactors = FALSE**)***. Reading the txt file containing land use types and keys: *land_use_keys <- **read.table(**file = "O:/Rscript/data/input/use_keys.txt", header = TRUE, sep = ",", stringsAsFactors = FALSE**)***. Reading the txt file containing columns of time since cultivation: time_since_cult <- ***read.table(**"O:/Rscript/data/input/time_since_cult.txt", header = TRUE, sep = "\t", stringsAsFactors = FALSE**)***. The read files from the current working directory by R can be seen in the global environment as shown in the table below:

TABLE 1 Reading files in R environment

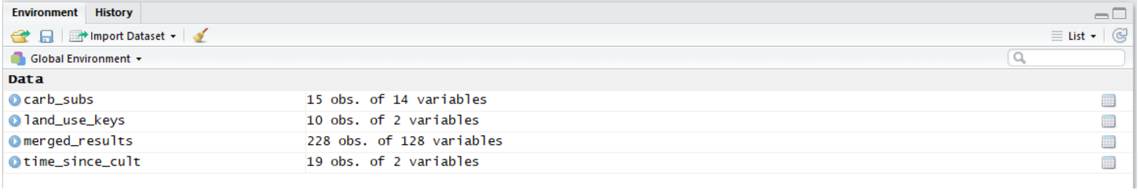

```
Data
carb_subs            15 obs. of 14 variables
land_use_keys        10 obs. of 2 variables
merged_results       228 obs. of 128 variables
time_since_cult      19 obs. of 2 variables
```

The needed files have been read by R, the next step is to combine those files into a target file for plotting graphs. As file “merged_results” has a rather complex content and form, hence the other two files “time_since_cult” and “carb_subs” can be combined at first. The txt file time_since_cult has the contents of time since cultivation in Finland, which is unnecessary for this work, therefore deleting FI part and assign the new data table with a new name: *time_since_cult1 <- time_since_cult**[-**c(1,2,3,4),**]***. Since file “time_since_cult” and file “carb_subs” have an overlapping column “site”, therefore the two files can be combined based on this overlapped column. Reordering the rows in file “time_since_cult” in order to have exactly a same column in file “carb_subs”: *time_since_cult_final <- time_since_cult1[c(6:9,1:5,10:15),]*. Combining files “time_since_cult_final” and “carb_subs” excluding the overlapping column “site”: *combined_data_1 <- **cbind(**carb_subs, time_since_cult_final[,2]**)***.

Combining the first two columns named "country" and "profil" in file “merged_results” into a new name "country profil" by using function: *merged_results$site <- **paste(**merged_results$country,merged_results$profil,sep=""**)***. Deleting the columns “country” and “profil” by assigning a NULL value to these two columns. Moving the last ID column “site” to the first column: *merged_results.new <- merged_results[,c(127,1:126)]*. Extracting columns "site"" and "use" and creating a new data frame:

*land_use1 <- **data.frame(**merged_results$site,merged_results$use**)***. Subsetting the necessary rows: *land_use2 <- **subset(**land_use1, merged_results.site %in% c("DEP1","DEP3", "EEP1", "EEP4", "EEP5", "EEP6", "EEP7", "DKP1", "DKP2", "DKP4", "DKP5", "NLSP1", "NLSP2", "NLSP3", "NLSP4")**)***. Creating a new data frame with the first appearance of each merged_results.site / use pair: *land_use3 <- land_use2**[!duplicated**(land_use2$merged_results.site),**]***. Reordering rows: *land_use4 <- land_use3[c(3:6,7:11,1:2,12:15),]*. Renaming columns: **colnames(**land_use4**)** <- c("Site","use"). Replacing ID column “site” values by column “site” in file “combined_data_1”: *land_use4[["Site"]]<- combined_data_1[["Site"]]*. In column “use’, the different numbers representing different land use types, in order to make the data table more compendious and clear, inputting the land use types represented by corresponding numbers, for instance number “1” represents land use type “igrass”, *land_use4$use[land_use4$use == "1"] <- "igrass"*.

Inserting column “use” in file “land_use4” into file “combined_data_1” to get the target file: *compiled_file <- **cbind(**combined_data_1, land_use4[,2]**)***. Outputting the “compiled_file” to the working directory: ***write.table**(compiled_file, file = "O:/Rscript/statistical plots and tables/compiled file.txt"**)***. Appendix 1 shows the compiled file for statistical plots.

Bar plotting

Creating a bar plot where X-axis represents the category of time since cultivation, Y-axis represents the median of carbon loss in each time since cultivation category, the error propagation is added to the bar plot as well. Firstly, grouping data of column “Cultivation_time” into three groups, which are “more than 100 years”, “fewer than 50years”, “between 50 and 100 years”, function **split()** can achieve this goal, *s1 <- **split(**compiled_file,compiled_file$Cultivation_time**)***. Combining the lists 52 and 50-100, so they are grouped into category “between 50 and 100”: *Bt_50_and_100 <- **rbind.data.frame(**s1$`52`,s1$` 50-100`**)***. Combining the lists 0 and 41, so they are grouped into category “less than 50”: *less_than_50 <- **rbind.data.frame(**s1$`0`,s1$`41`**)***. Creating a new list containing 3 data sets, which are less than 50, between 50 adn 100, more than 100: *target_file <- **list(**less_than_50,Bt_50_and_100,s1$` more than 100`**)***. *R*enaming the data sets in the list: ***names(**target_file**)** <- c("less than 50","between 50 and 100","more than 100")*.

Secondly, finding out the median of carbon loss and error propagation in each data list. Function **median()** can be used to find the median value, for instance, *m1 <- **median(**target_file$`less than 50`$CLoss.kg_m2**)***, m1 represents the median value of carbon loss in a category fewer than 50years of cultivation. Therefore, m2 and m3 representing the median value of carbon loss can be found by using the same method. A vector containing the three values can be created: *C_Loss_kg_m2.m <- c(m1,m2,m3)*. The equation below shows the equation of error propagation,

$$\Delta \mathrm{X} = \frac{\sqrt{\sum x^2}}{n} \tag{11}$$

Where,
ΔX is the error propagation
x represents all values involved
n is the length of columns, which is the number of values involved.

The length of column “CLoss.kg_m2_sem” can be found by using function **length()**, for instance, the length of column “CLoss.kg_m2_sem” in data list fewer than 50years can be found by using: *n1 <- **length(**target_file$`less than 50`$CLoss.kg_m2_sem**)***. The error propagation can be calculated by employing the equation above: *delta_x1 <- sqrt(sum((target_file$`less than 50`$CLoss.kg_m2)^2))/n1*. The error propagation *delta_x2* and *delta_x3* of data lists “between 50 and 100 years” and “more than 100 years” can be found out by using the same method. Therefore, a vector containing values of error propagation can be created: *delta_x <- c(delta_x1, delta_x2, delta_x3)*.

Thirdly, making bar plots and adding error propagation on the bars. Outputting the plot as a pdf file in the current working directory: ***pdf("****O:/Rscript/statistical plots and tables /Carbon Loss VS. Time Since Cultivation.pdf****")***, so that bar plots can be saved automatically, manual extraction of plots is not necessary. Creating a bar plot, defining an object mids and give the bar plot value to mids in order to determine the x_0 value while adding error propagation on the bars.

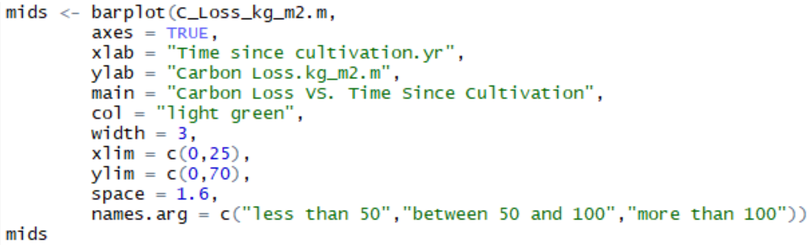

```
mids <- barplot(C_Loss_kg_m2.m,
        axes = TRUE,
        xlab = "Time since cultivation.yr",
        ylab = "Carbon Loss.kg_m2.m",
        main = "Carbon Loss VS. Time Since Cultivation",
        col = "light green",
        width = 3,
        xlim = c(0,25),
        ylim = c(0,70),
        space = 1.6,
        names.arg = c("less than 50","between 50 and 100","more than 100"))
mids
```

FIGURE 4 Creating a bar plot of cultivation time associated with carbon loss

Adding the error propagation onto the bar plots by using **arrows()** function: ***arrows(****mids, C_Loss_kg_m2.m-(delta_x)/2,mids, C_Loss_kg_m2.m+(delta_x)/2, code = 3, angle = 90, length = 0. 1****)***, wherein, *mids* defines the starting point of the error bars on X-axis, *C_Loss_kg_m2.m-(delta_x)/2* determines the length of error bars in the downward direction, *C_Loss_kg_m2.m+(delta_x)/2* determines the length of error bars in the upward direction. Returning the output to the terminal by using function **dev.off( )**. The bar plot of carbon loss in response to time since cultivation can be seen in the chapter of results of this work.

Plotting the carbon loss among various land use types

The land use types in the researching sites are intensively managed grassland, paludiculture land, peat extraction land, pasture land, wheat land, extensively managed grassland, and barley land. Wherein intensively managed grassland, extensively managed grassland, pasture land is considered as grassland, barley and wheat are considered as arable land, rewetted land and extraction land is considered neither of the two land use type categories.

Classifying the land use types into two categories, which are grassland and arable land. Firstly, using function **split()** to group the column “use” in file “compiled_file” into several different data lists : *s_use <-* ***split(****compiled_file, compiled_file$Use_type****)***. Secondly, classifying egrass, igrass and pasture into the category of grassland by using function **rbind.data.frames()**:*Grassland <* ***rbind.data.frame(****s_use$egrass,s_use$igrass,s_use$pasture****)***. Classifying barley and wheat into category arable land: *Arable land <-* ***rbind.data.frame(****s_use$barley,s_use$wheat****)***. Thirdly, finding out the median value of carbon loss in the data list of grassland: *CLoss.m_g <-* ***median(****Grassland$CLoss.kg_m2****)***, and the median of carbon loss in the data list of arable land: *CLoss.m_a <-* ***median(****Arableland$CLoss.kg_m2****)***. Then, finding out the error propagation of the standard error of the median of carbon loss, assigning the error propagation of data list grassland to delta_g: *delta_g <-* ***(sqrt(sum(****(Grassland$CLoss.kg_m2_sem)^2****)))****/* ***length(****Grassland$CLoss.kg_m2_sem****)***, and delta_a represents the error propagation of the standard error of the median of carbon loss in category arable land: *delta_a <-* ***(sqrt(sum(****(Arableland$CLoss.kg_m2_sem)^2****)))/length(****Arableland$CLoss.kg_m2_sem****)***. Creating a vector containing the median of carbon loss from grassland and arable land: *CLoss.m <- c(CLoss.m_g,CLoss.m_a)*. Creating a vector containing the error propagation of data list grassland and arable land: *delta.use <- c(delta_g,delta_a)*. outputting the bar plot as a pdf file to the terminal folder: ***pdf(***"*O:/Rscript/statistical plots and tables /Carbon Loss in Comparison with Land Use Type.pdf*"***)***. Defining the object Mids in order to determine the error propagation bar on the bar plots, the bar plot of carbon loss among different land use types can be generated by using function **barplot()**, as shown in the figure below.

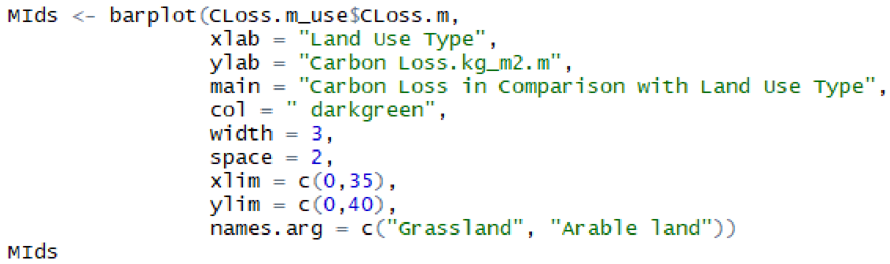

```
MIds <- barplot(CLoss.m_use$CLoss.m,
                xlab = "Land Use Type",
                ylab = "Carbon Loss.kg_m2.m",
                main = "Carbon Loss in Comparison with Land Use Type",
                col = " darkgreen",
                width = 3,
                space = 2,
                xlim = c(0,35),
                ylim = c(0,40),
                names.arg = c("Grassland", "Arable land"))
MIds
```

FIGURE 5 Creating a bar plot of land use associated with carbon loss

Adding the error whiskers of the median of carbon loss onto the bar plot by using function **arrows()**: ***arrows(****MIds, CLoss.m_use$CLoss.m-(delta.use)/2,MIds, CLoss.m_use$CLoss.m+(delta.use)/2, code = 3, angle = 90, length = 0.1,col = "blue"****)***. Returning the output to the terminal folder by using function **dev.off()**. Therefore, the bar plot of "Carbon Loss in Comparison with Land Use Type" is generated.

Plotting the carbon loss associated with land types and cultivation time

The lists in "target_file" created while generating bar plots of carbon loss in response to time since cultivation category are grouped based on the category of land use types. In the data list "less than 50", there are three land use types, which are extraction, igrass and barley, grouping igrass to the grassland group and barley to the arable land group. In the data list "between 50 and 100", there are two land use types, which are igrass and wheat, igrass is classified to the category of grassland, wheat is classified to the category of arable land. In data list "more than 100", land use types of rewetted, egrass and pasture are included, egrass and pasture belonging to group grassland while rewetted belongs to the noun of them.

To generate the bar plot, the median value of carbon loss from grassland and arable land in each data list should be found out first. For instance, firstly, grouping land use types in data list "less than 50" by using function: *s_less_50 <-* ***split(****target_file$`less than 50`, target_file$`less than 50`$Use_type****)***, then classify land use type "igrass" to the category grassland: *g_less_50 <-* ***data.frame(****s_less_50$igrass****)***, and land use type "barley" to the category arable land: *a_less_50 <- s_less_50$barley*. Finding out the median of carbon loss from grassland and arable land: *g_less_50.m <-* ***median(****g_less_50$CLoss.kg_m2****)***, *a_less_50.m <-* ***median(****a_less_50$CLoss.kg_m2****)***. Finding out the error propagation of all median values of carbon loss: *g_less_50.delta <-* ***(sqrt(sum(****(g_less_50$CLoss.kg_m2_sem)^2)****))****/* ***length(****g_less_50$CLoss.kg_m2_sem****)***, *a_less_50.delta <-* ***(sqrt(sum(****(a_less_50$CLoss.kg_m2_sem)^2)****))****/****length(****a_less_50$CLoss.kg_m2_sem****)***. Wherein, *g_less_50.delta represents the error propagation in category grassland and* a_less_50.delta represents the error propagation in category arable land.

By following the same method, the median of carbon loss from both grassland and arable land can be found in data list “between 50 and 100” and “more than 100”, as well as the error propagation. Creating a vector which contains the median of carbon loss from grassland and arable land in each data list: *median_c_loss <- c(g_less_50.m,a_less_50.m,g_bt.50_100.m,a_bt.50_100.m,g_more_100.m,a_more_100.m)*. Creating a vector containing the error propagation for each median of carbon loss: *delta <- c(g_less_50.delta,a_less_50.delta,g_bt.50_100.delta,a_bt.50_100.delta,g_more_100.delta,a_more_100.delta)*. Outputting the bar plot in a pdf file in the terminal folder: ***pdf("****:/Rscript/statistical plots and tables/Carbon Loss VS. Time Since Cultivation in Comparison of Land Type.pdf****")***. Defining an object “MIDs” for adding error propagation onto the bars in the plot and creating the bar plot, as shown in the figure below.

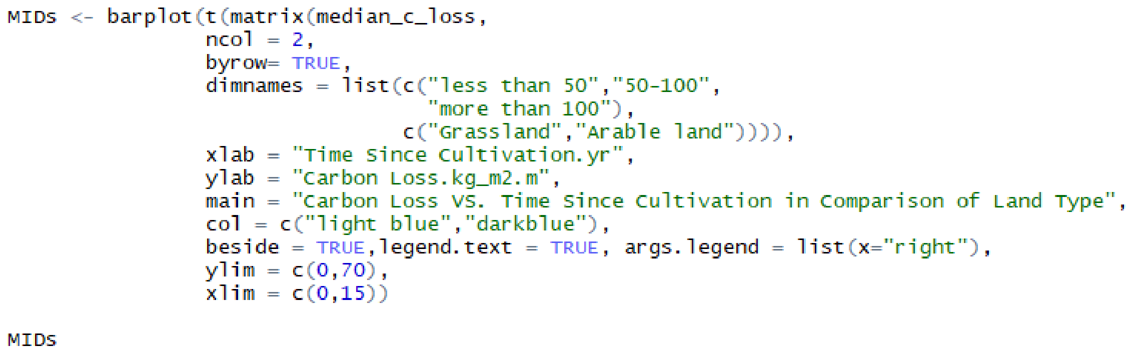

```
MIDs <- barplot(t(matrix(median_c_loss,
                ncol = 2,
                byrow= TRUE,
                dimnames = list(c("less than 50","50-100",
                                  "more than 100"),
                                c("Grassland","Arable land")))),
                xlab = "Time Since Cultivation.yr",
                ylab = "Carbon Loss.kg_m2.m",
                main = "Carbon Loss VS. Time Since Cultivation in Comparison of Land Type",
                col = c("light blue","darkblue"),
                beside = TRUE,legend.text = TRUE, args.legend = list(x="right"),
                ylim = c(0,70),
                xlim = c(0,15))

MIDs
```

FIGURE 6 Creating a bar plot

Adding the error propagation onto the bars: ***arrows(****MIDs,median_c_loss-(delta/2), MIDs,median_c_loss+(delta/2), code = 3, angle = 90, length = 0.05****)***. Returning the output to the terminal folder by using function **dev.off()**.

Plotting variables influencing the decomposition rate

Microbes break down organic matters in soils at an aerobic condition, during this process carbon dioxide is produced and released to the atmosphere, which is significant to be taken into account while analyzing the influences of cultivation time and land use types on carbon losses from organic soils.

In order to plot the graph showing the carbon loss in response to a variety of variables, the first step is to read files containing all necessary information. In this situation, all of the information on decomposition, pH value, temperature, C/N ratio, drainage types, and water tables are contained in one file, as mentioned above, function **read.table()** can fulfil this objective. Then manipulate the file to the one only containing the demanded information. Thereby, extracting the entire columns of "site", "decomposition", "pH.CaCl2.", "CN.median", "drain", "T_degC_median", "gwh_m_median", "Hrtop", "Hwtop" and creating a new data frame by using function **data.frame(**data file, columns). Then extracting the required rows and create another data frame. For instance, *new.data1 <-* ***subset(****new.data, new.data$merged_results.new.site* ***%in%*** *c("DEP1","DEP3", "EEP1", "EEP4", "EEP5", "EEP6", "EEP7", "DKP1", "DKP2", "DKP4", "DKP5", "NLSP1", "NLSP2", "NLSP3", "NLSP4")****)***. As multiple rows appear with the same identity and contents, the first appearance in rows needs to be extracted by employing function *new.data.2 <- new.data1****[!duplicated(****new.data1$merged_results.new.site****),]***. The column names can be changed by using function **colnames ()**. The rows can be reordered as well in order to be consistent with the previous *"compiled_file",* for instance, *new.data3 <- new.data.2[c(3:6,7:11,1:2,12:15),]*. Replacing the ID column "site" by the "site" column in the file named as *compiled_file* by using *new.data3[["Site"]]<- compiled_file[["Site"]]*. Insert the carbon loss column and its standard error of the median column to the current data frame: *variables.df <-* ***cbind(****new.data3,compiled_file$ CLoss.kg_m2_sem, compiled_file$CLoss.kg_m2****)***. Therefore, *variables.df* is the target file for this task. In the end, replace all the "-9999" values to NA: *variables.df[variables.df == -9999]<- NA*.

Saving the plots directly in a pdf file: ***pdf(****"D:/Thesis/data/statistical analysis/factors influencing microbial activities in response to carbon loss.pdf"****)***. Multiple pictures are aimed to be created in one plot, using **layout (matrix ())** function to achieve this goal. For instance, the figure below shows the layout of the plot with 3 rows and 3 columns, wherein, the first row contains two columns and the array of pictures is arranged by rows.

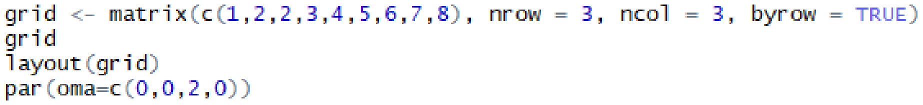

```
grid <- matrix(c(1,2,2,3,4,5,6,7,8), nrow = 3, ncol = 3, byrow = TRUE)
grid
layout(grid)
par(oma=c(0,0,2,0))
```

FIGURE 7 Layout of the plot

In order to generate the plot of factor of decomposition in response to carbon loss, using function: ***plot(****variables.df$decomposition,variables.df$`compiled_file$CLoss.kg_m2`,xlab = "Decomposition", ylab = "Carbon Loss. kg_m2",col = "red",col.main = "darkgrey",pch = 5****)***. Where the values of X-axis and Y-axis are defined, as well as the color and the symbol of the plot. Then generate a linear regression model of the two variables with the **lm()** function, and draw a trend line with **abline() function**.

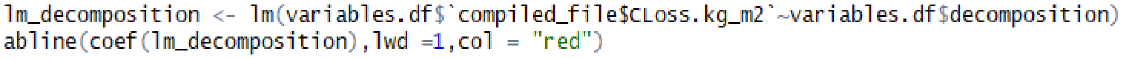

```
lm_decomposition <- lm(variables.df$`compiled_file$CLoss.kg_m2`~variables.df$decomposition)
abline(coef(lm_decomposition),lwd =1,col = "red")
```

FIGURE 8 Generation of a linear regression model in R

Eventually, the error bar is added to the plot by using **arrow()** function, as shown in the figure below. Plotting the other variables in response to carbon loss can be fulfilled by following the same method.

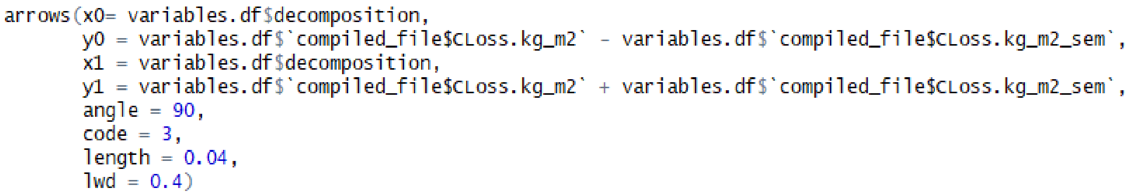

```
arrows(x0= variables.df$decomposition,
       y0 = variables.df$`compiled_file$CLoss.kg_m2` - variables.df$`compiled_file$CLoss.kg_m2_sem`,
       x1 = variables.df$decomposition,
       y1 = variables.df$`compiled_file$CLoss.kg_m2` + variables.df$`compiled_file$CLoss.kg_m2_sem`,
       angle = 90,
       code = 3,
       length = 0.04,
       lwd = 0.4)
```

FIGURE 9 Adding the error bar on the plot

3 RESULTS

3.1 Results of bulk density and Loi obtained from the laboratory

Bulk density (BD) refers to the dry mass per unit volume of soil, it is usually measured in units of grams per cubic centimeters (g/cm^3). Bulk density is one of the soil physical properties, directly indicating the quantity of soil pore space in a certain soil horizon. The larger amount of the space, the lower value of bulk density, which can be seen in the equation below:

$$\text{Pore space} = [1 - (\text{bulk density})/(\text{particle density})] * 100\% \qquad (12)$$

The particle density of mineral soil materials is higher than organic soil materials, as for the same volume of mineral and organic soil materials, the organic soil materials have a smaller mass than mineral soil materials, thus mineral soils are “heavier” than organic soils. In general, the average particle density of mineral soil materials is 2,65 g/cm^3 , while the average particle density of organic soil materials is 1,25 g/cm^3. Therefore, adding organic soil materials to the mineral soil materials can lower its bulk density. Bulk density is inversely proportional to the number of organic soil materials, the lower bulk density indicates a higher amount of organic soil materials in the soil composition. (USDA. 2014)

Loss of ignition is used to directly estimate the organic matter content in soils. Ignition of soils converts the organic matter into CO_2, the remaining ash residue is the inorganic compounds contained in soils. Even though the loss of ignition method is widely employed in order for the measurement of organic matter content worldwide, there are factors that may affect its accuracy, for instance, the type of furnace, the ignition temperature and ignition time, the mass of samples, the duration of stay in desiccators, the clay content in samples, as well as the individual-dependent manual operations. (M.J.J.Hoogsteen, et al. 2015)

The obtained results of bulk density and loss of ignition from the quadruplicate experiments are shown from FIGURE 10 to FIGURE 24 (A. Piayda & L. Sokolowsky. 2017) in this section, which are marked in filled diamond shape with different letters (A, B, C, D) and colors (red, green, blue, purple), wherein the average of the four profiles is marked as “avg” in black color in both graphs. Among all figures, the left graph always shows acquired results of bulk density, while the right graph always indicates results of loss of ignition. Y-axis represents the soil core depth in unit centimeter (cm), the range of soil core depth is from 0 cm to 100 cm (from the surface ground to underground). X-axis represents the bulk density in unit grams per cubic centimeters (g/cm^3) and the loss of ignition with decimals, the range of values is from 0 to 1.

3.1.1 Denmark

FIGURE10 shows the bulk density and loss of ignition at the first site geographically located at N 56°27', E 9°40' in Denmark. On the left graph, the bulk density obtained from four trials are almost identical from depth 0 to 50 cm, the values relatively do not differ much. However, from around 50 cm to 100 cm depth, the similarity starts to change, the values of bulk density differ very much among all four profiles. The values from each profile have a different trend. From 0 to around 18 cm depth underground, the bulk density is increasing from 0,28g/cm^3 to 0,40 g/cm^3. Then, the bulk density is decreasing to around 0,21 g/cm^3 from 18 cm to 54 cm depth underground. From 54 cm to 100 cm depth, alternates between increase and decrease.

On the right graph, the values of Loi from two trials are quite similar, from 0 cm to around 18 cm, they tend to decrease from 0,78 to 0,75, while from 18 cm to 69 cm, they tend to increase from 0,75 to around 0,83. From 0 cm to 18 cm depth underground, the value from the other one profile (blue) is increasing from around 0,62 to 0,71, while the values from another profile (purple) are almost not changing and stay at around 0,72. From 18 cm to 21 cm depth, the value of Loi in the profile marked with blue color is decreasing to around 0,60 and from 21 cm to 48 cm depth, the value is increasing to around 0,79. However, the value decreases to around 0,3 at depth 60 cm and increases to around 0,84 at depth 87 cm. Within the range of depth from 0 cm to 18 cm, the average values of Loi tend to be the same as one of the trails (purple) and stay at around 0,73, from 18 cm to 21 cm, the value decreases to around 0,70. From 21 cm to 48 cm, the average value of Loi tends to increase from 0,73 to around 0,82. From 48 cm to 81 cm, the average of Loi reaches the lowest value of 0,42. From 81 cm to 100 cm, the average of Loi increases to around 0,58. Thereby, the overall trend of the average of Loi is decreasing from around 0,72 to around 0,58.

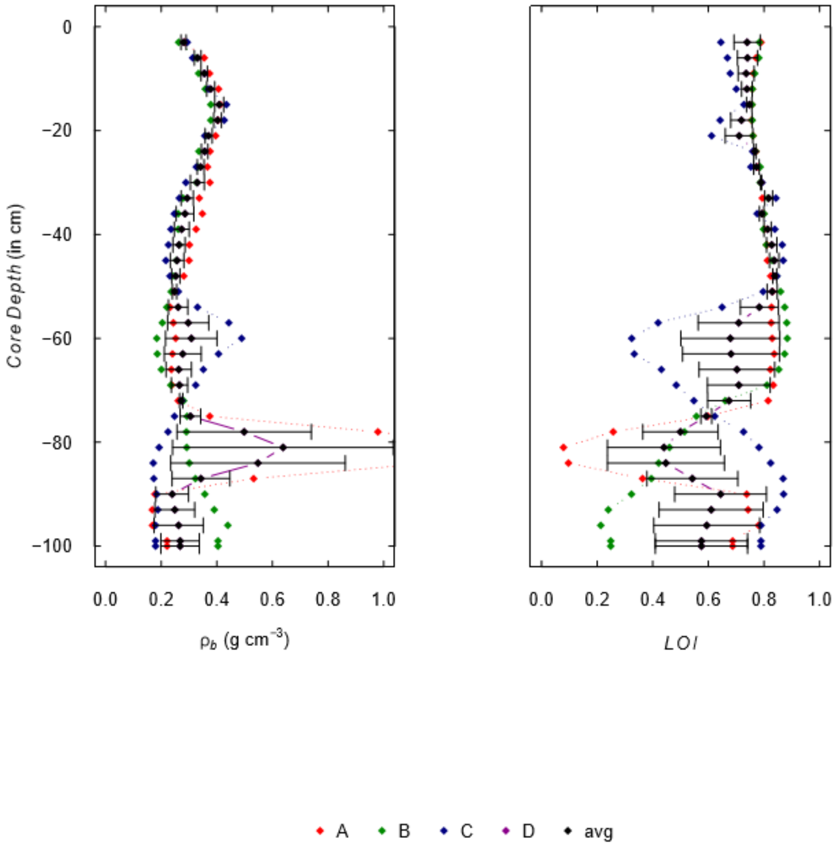

FIGURE 10 Bulk density and Loi at the first site in Denmark (N 56°27', E 9°40')

In FIGURE 11, the results of bulk density and Loi obtained at the second site in Demark are provided. On the left graph, the results obtained from four trails are quite similar and they tend to have the same trends, which from 0 cm to 24 cm depth, the bulk density is increasing from around 0,26 g/cm^3 to 0,38 g/cm^3 in average, from 24 cm to 100 cm, the average values of bulk density are decreasing, wherein, from 24 cm to 36 cm depth, the values decrease from 0,38 g/cm^3 to 0,28 g/cm^3, from 36 cm to 100 cm, the decreasing rate is slower, the average value of bulk density reaches to around 0,18 g/cm^3.

On the right graph, the average of Loi is decreasing from 0 cm to 6 cm, along with the value changes from 0,78 to 0,76. From 6 cm to 33 cm depth, the average value is increasing and reaching to 0,83. From 33 cm to 54 cm depth, the average of Loi is almost not changing. From 54 cm to 60 cm depth, the average of Loi is slightly decreasing to 0,81 due to the value from one trial (blue) was decreasing, and within this range of depth, the values of Loi from the trial marked with blue color differs the most from the other trials. From 60 cm to 66 cm depth, the average of Loi increases back to around 0,83. From 66 cm to 100 cm, the average value of Loi is almost not changing, within this range of depth, the results from all trials are very consistent.

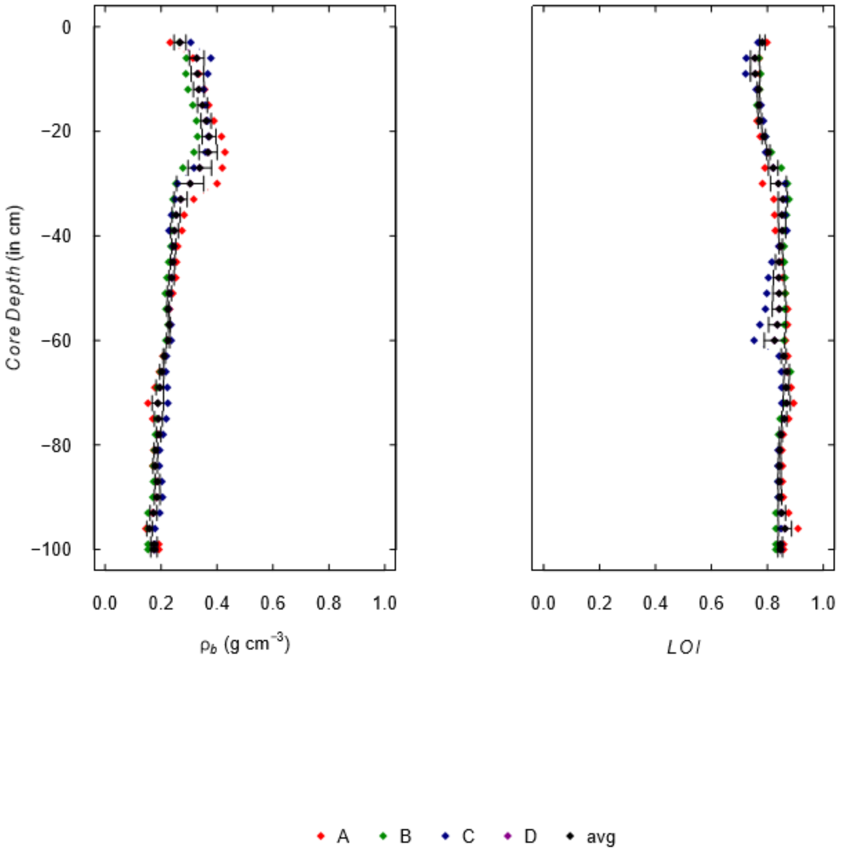

FIGURE 11 Bulk density and Loi at the second site in Denmark (N 56°27', E 9°40')

FIGURE 12 indicates the acquired results of bulk density and Loi at the third site in Denmark. In general, the results from all trials are very homogeneous and almost stay at the same values per depth. On the left graph, from 0 cm to 18 cm depth, the average value of bulk density is increasing from 0,12 g/cm^3 to 0,36g/cm^3. From 18 cm to 45 cm depth, the average of bulk density decreases to 0,16 g/cm^3. From 45 cm to 57 cm depth, the average value slightly increases to 0,17 g/cm^3 . From 57 cm to 96 cm, the average value is gradually decreasing until it reaches around 0,11 g/cm^3 . From 96 cm to 100 cm, the average value is sharply decreasing to around 0,08 g/cm^3 due to the values of Loi from one trail (red) at depth 99cm and 100 cm are zero.

On the right graph, from 0 cm to 15 cm, the average value of Loi is decreasing from around 0,89 to around 0,78. From 15 cm to 45 cm, the average value of Loi is increasing to around 0,89. From 45 cm to 60 cm, the average value of Loi is decreasing to around 0,86. From 60 cm to 100 cm, the average value of Loi is very slightly increasing to around 0,88. The curve is almost vertical within the range of depth from 60 cm to 100 cm.

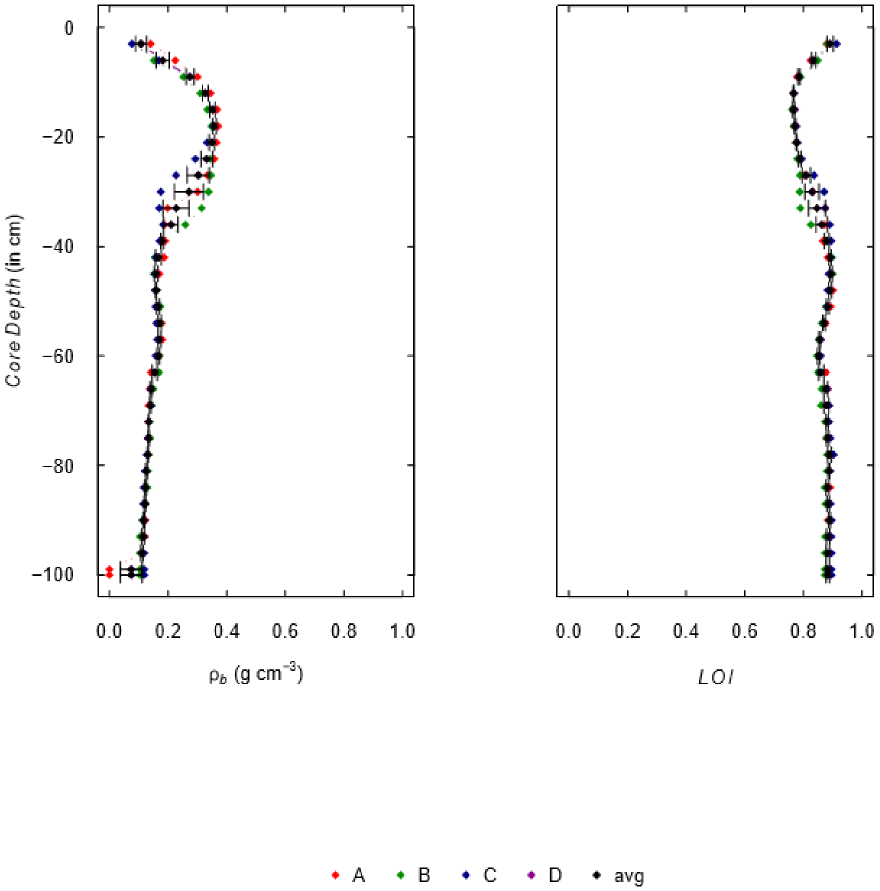

FIGURE 12 Bulk density and Loi at the third site in Denmark (N 56°29', E 9°51')

FIGURE 13 shows the values of bulk density and Loi at the fourth site in Denmark. Overall, from 0 cm to 66 cm, the values of bulk density and Loi per depth obtained from all profiles are quite homogenous. From 66 cm to 100 cm depth, there are great differences among all trials. In addition, the two graphs of bulk density and Loi are seem to be as mirror graphs, which the Y-axis is the central axis, although this description may not be very accurate while looking at the corresponding values at each depth. Within the range of depth that the average values of bulk density increases, the average of Loi decreases, the same situation that within a certain range of depth, the average value of Loi increases while the average value of bulk density decreases.

On the left graph, the average of bulk density is increasing from 0,18 g/cm^3 to 0,38 g/cm^3 within the first 9 cm of depth, while the value is decreasing and reaching to 0,17 g/cm^3 at depth 42 cm. From 42 cm to 54 cm, the average of bulk density is slightly increasing to 0,18 g/cm^3 . While the value is decreasing to around 0,14 g/cm^3 again at 66 cm depth.

On the right graph, from 0 cm 9 cm depth, the average value of Loi is decreasing from 0,82 to around 0,77, while the value is increasing and reaching to around 0,89 at depth 30cm. from 30 cm to 42 cm, the average value of Loi is almost not changing, while from 42 cm to 54 cm, the average of Loi is slightly decreasing from around 0,89 to 0,87. From 54 cm to 66 cm, the average of Loi is slightly increasing to 0,89.

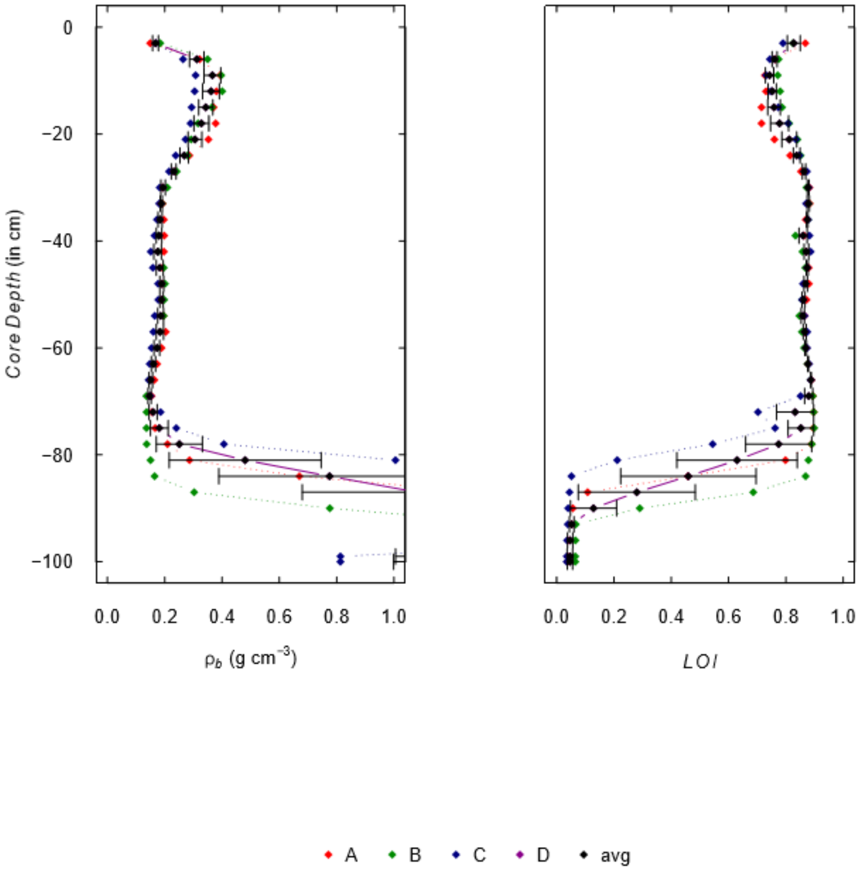

FIGURE 13 Bulk density and Loi at the fourth site in Denmark (N 56°29', E 9°51')

3.1.2 Estonia

In FIGURE14, the values of bulk density and Loi from all trials are quite the same, the obvious increase or decrease cannot be seen in both graphs. However, the average bulk density is slightly increasing from 3 cm to 6 cm, the difference stays within around 0,01. rom 6 cm to 12 cm, the bulk density stays at the same value of around 0,16 g/cm^3. From 12 cm to 39 cm, the average of bulk density is very slightly decreasing to 0,12 g/cm^3. From 39 cm to 51 cm, the average of bulk density is gradually increasing to 0,16 g/cm^3.

From 51 cm to 63 cm, the value is decreasing to 0,15 g/cm^3, while from 63 cm to 84 cm, the average of bulk density is increasing to 0,17 g/cm^3. From 84 cm to 100 cm, the average of bulk density stays at the same value of 0,17 g/cm^3. The values of Loi stays at around 0,98 within the 1 m depth, the curve is vertical.

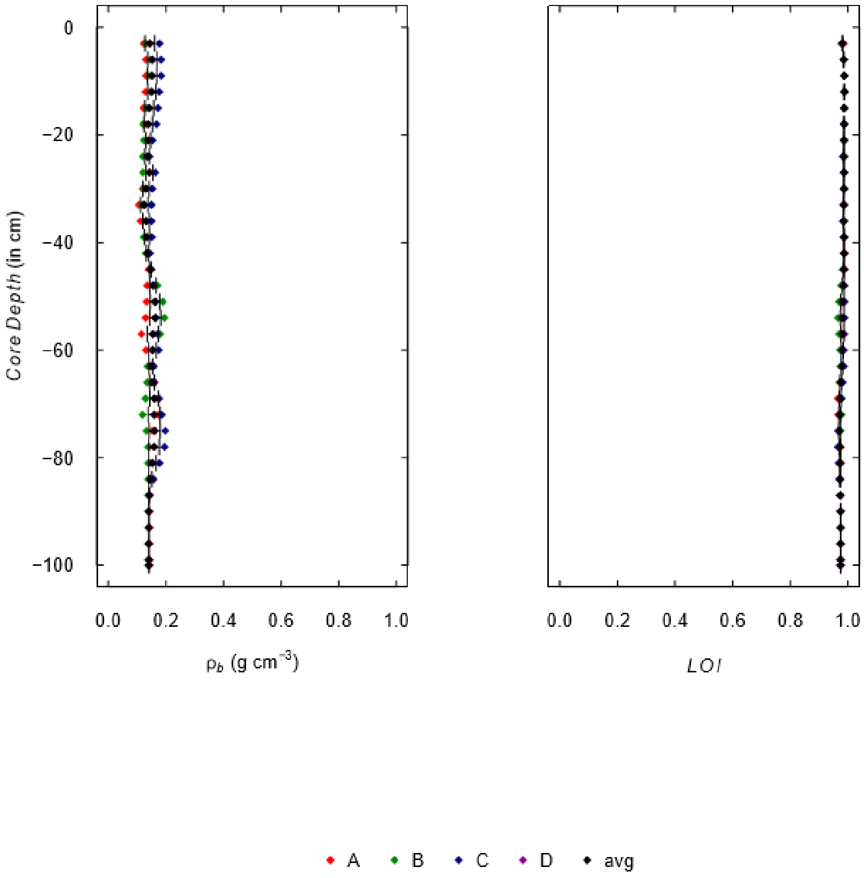

FIGURE 14 Bulk density and Loi at the first site in Estonia (N 58°30', E 27°0')

In FIGURE 15, on the left graph, the bulk density increases from 0 cm to 21 cm and reaches the maximum value of 0,43 g/cm^3, from 21 cm to 84 cm, the average of bulk density is decreasing and reaching to the minimum value of 0,20 g/cm^3. From 84 cm to 100 cm, the value is slightly increasing to around 0,22 g/cm^3. On the right graph, from 0 cm to 15 cm depth, the average value of Loi is decreasing from 0,64 to 0,57. From 15 cm to 87 cm, the average of Loi is increasing and reaching a maximum value of 0,91. From 87 cm to 100 cm, the average of Loi is decreasing to around 0,88.

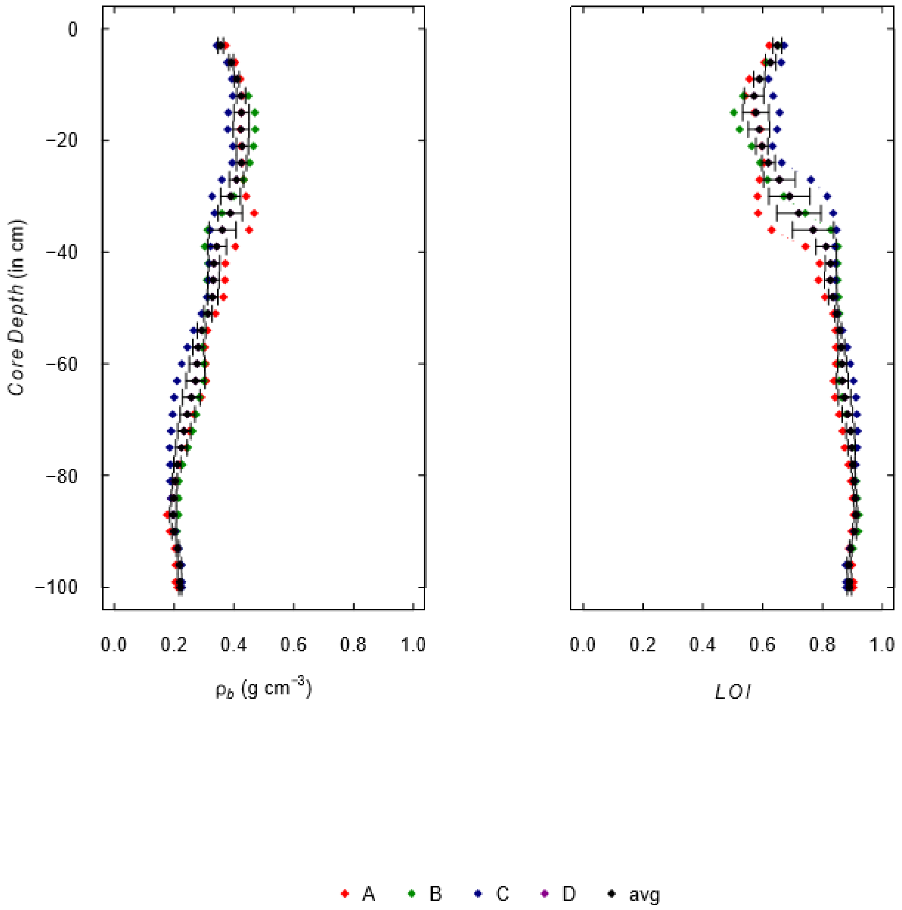

FIGURE 15 Bulk density and Loi at the second site in Estonia (N 58°15', E 26°9')

In FIGURE 16, on the left graph, from 0 cm to 9 cm, the average of bulk density is slightly increasing and reaching the maximum value of 0,39 g/cm^3 at depth 9 cm underground. From 9 cm to 18 cm, the value stays the same. From 18 cm to 66 cm, the average of bulk density is decreasing to around 0,19 g/cm^3, while from 66 cm to 100 cm depth, the value is gradually increasing to around 0,23 g/cm^3. On the right graph, from 0 cm to 6 cm, the average value of Loi is slightly decreasing and the difference is within 0,01. From 6 cm to 15 cm, the value is slightly increasing from around 0,70 to 0,74, from 15 cm to 21 cm, the average of Loi is decreasing again to around 0,73 and from 21 cm to 66 cm, the value is increasing to 0,91. From 66 cm to 100 cm, the average of Loi is decreasing to around 0,89.

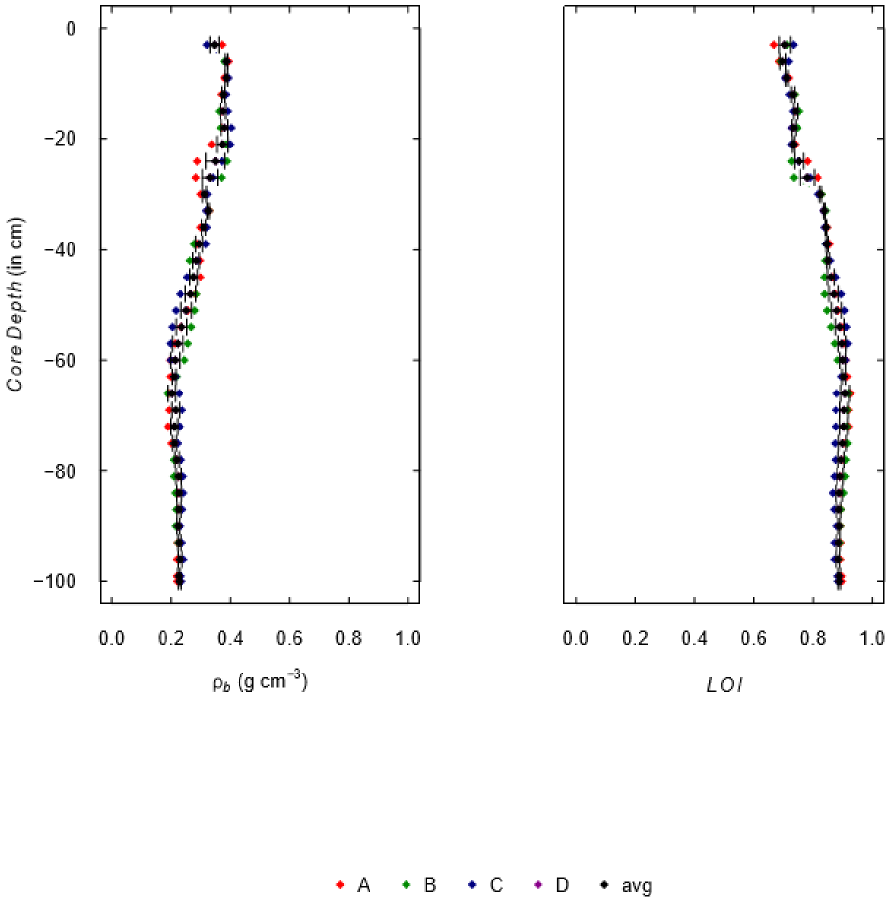

FIGURE 16 Bulk density and Loi at the third site in Estonia (N 58°15', E 26°9')

In FIGURE 17, on the left graph, from 0 cm to 18 cm depth, the average of bulk density increases from around 0,14 g/cm^3 to around 0,28 g/cm^3. While from 18 cm to 75 cm depth, the value is decreasing to around 0,18 g/cm^3. The decreasing rate from 18 cm to 30 cm is rather fast, while the value is slightly decreasing from 30 cm to 66 cm, from 66 cm to 75 cm, the average of bulk density decreases from around 0,29 g/cm^3 to around 0,19 g/cm^3. From 75 cm to 100 cm, the values of bulk density vastly increase. On the right graph, from 0 cm to 12 cm depth, the average value of Loi decreases from around 0,74 to around 0,70. While from 12 cm to 42 cm depth, the value increases to 0,84. From 42 cm o 51 cm, the average of Loi does not change much, from 54 cm to 69 cm, the value increases to around 0,87. From 69 cm to 78 cm, the value decreases to around 0,83. From 78 cm to 87 cm, the average of Loi sharply decreases to around 0,01. From 87 cm to 100, the value does not change much but stays at around 0,01.

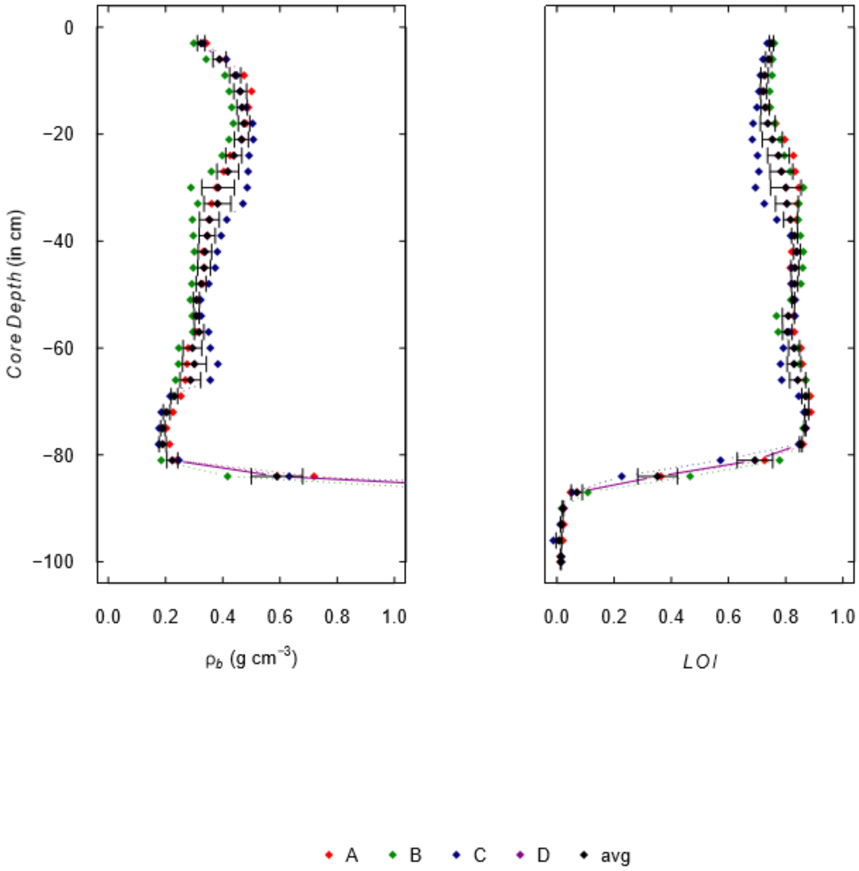

FIGURE 17 Bulk density and Loi at the fourth site in Estonia (N 58°13', E 26°17')

FIGURE 18 shows the values of bulk density and Loi from a barley land site in Estonia. On the left graph, from 0 cm to 15 cm depth, the average value of bulk density increases from around 0,35 g/cm^3 to around 0,45 g/cm^3. While from 15 cm to 93 cm depth, the value gradually decreases to around 0,18 g/cm^3. On the right graph, from 0 cm to 42 cm, the average of Loi gradually increases from around 0,73 to around 0,83. From 42 cm to 63 cm, the value decreases to around 0,82. From 63 cm to 81 cm, the average of Loi slightly increases to around 0,83. From 81 cm to 91 cm, the average of Loi gradually decreases from around 0,83 to 0,82. While from 91 cm to 100 cm, the value sharply decreases to around 0,21.

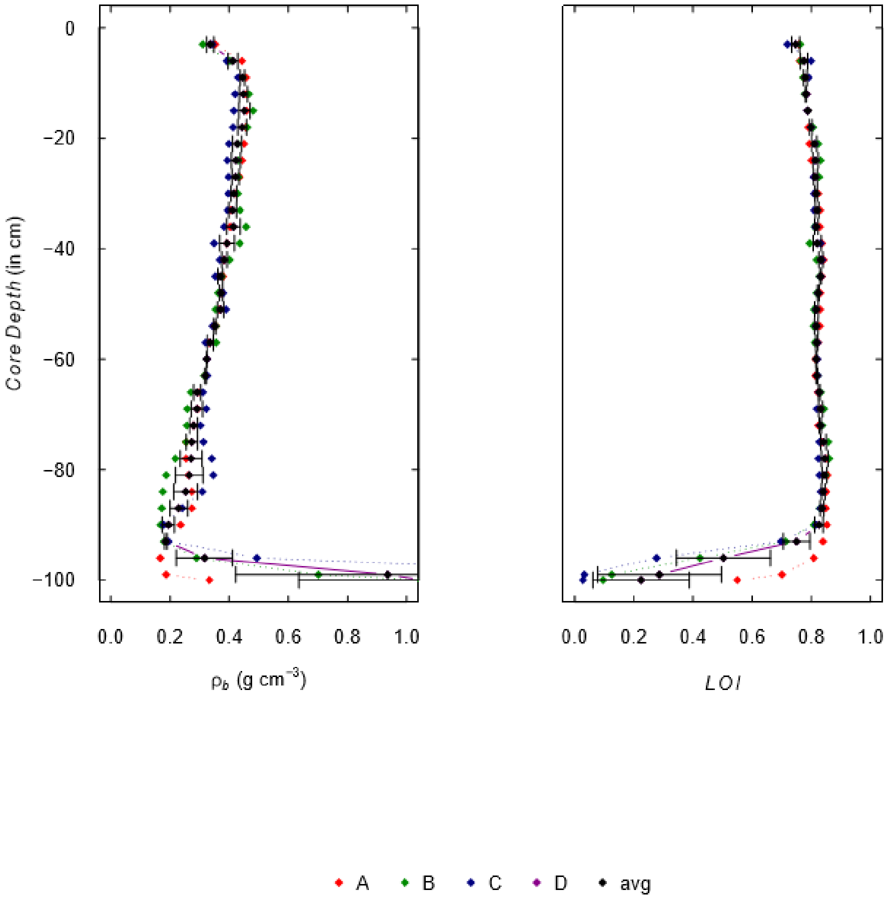

FIGURE 18 Bulk density and Loi at the fifth site in Estonia (N 58°13', E 26°17')

3.1.3 Germany

In FIGURE 19, from 0 cm to 18 cm, the average of bulk density increases from approximately 0,38 g/cm^3 to approximately 0,43 g/cm^3. Then the value decreases to approximately 0,21 g/cm^3 within the depth range of 18 cm and 63 cm. from 63 cm to 87 cm, the average of bulk density increases and then decreases until 100 cm depth.

On the right graph, from 0 cm to 6 cm depth, the average of Loi increases from approximately 0,71 to around 0,78. From 6 cm to 15 cm, the average of Loi stays at the same value, while from 15 cm to 27 cm, the average of Loi increases to around 0,83. From 27 cm to 33 cm, the value decreases to around 0,81. From 27 cm to 78 cm, the average value of Loi gradually increases to approximately 0,88. From 78 cm to 90 cm, the value sharply decreases to approximately 0,48 then the value increases to approximately 0,67 at 99 cm depth.

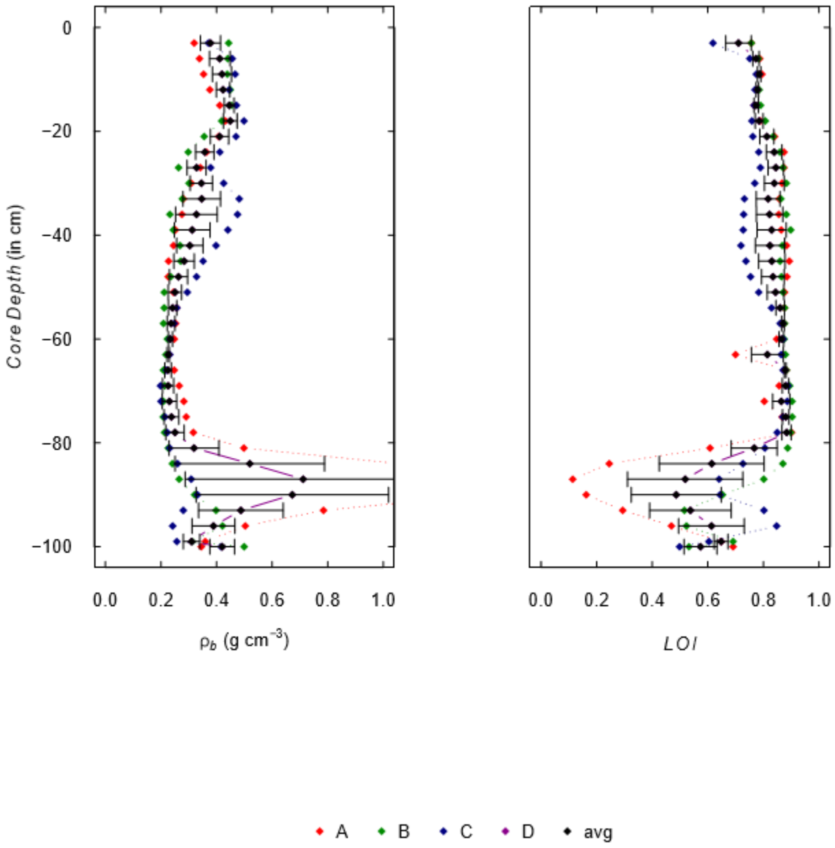

FIGURE 19 Bulk density and Loi at the first site in Germany (N 48°30', E 10°15')

In FIGURE 20, the values of bulk density increase from approximately 0,2 g/cm^3 to 0,29 g/cm^3 starting from the ground surface down to 9 cm depth. Then the value decreases to around 0,18 g/cm^3 from 9 cm to 24 cm depth. From 24 cm to 69 cm depth, the average of bulk density gradually decreases to approximately 0,14 g/cm^3. From 69 cm to 90 cm, the average of bulk density increases to approximately 0,42 g/cm^3 and then sharply decreases to approximately 0,02 g/cm^3 at 100 cm depth.

Within the range of depth at the first 9 cm of the soil core, the average of Loi slightly decreases from 0,77 to around 0,77, then the value increases to approximately 0,89 within the range of depth from 9 cm to 33 cm. from 33 cm to 69 cm, the average value of Loi does not change and stays at a value of 0,89. From 69 cm to 90 cm depth, the average of Loi sharply decreases to approximately 0,32. From 90 cm to 100 cm depth, the value almost stays the same.

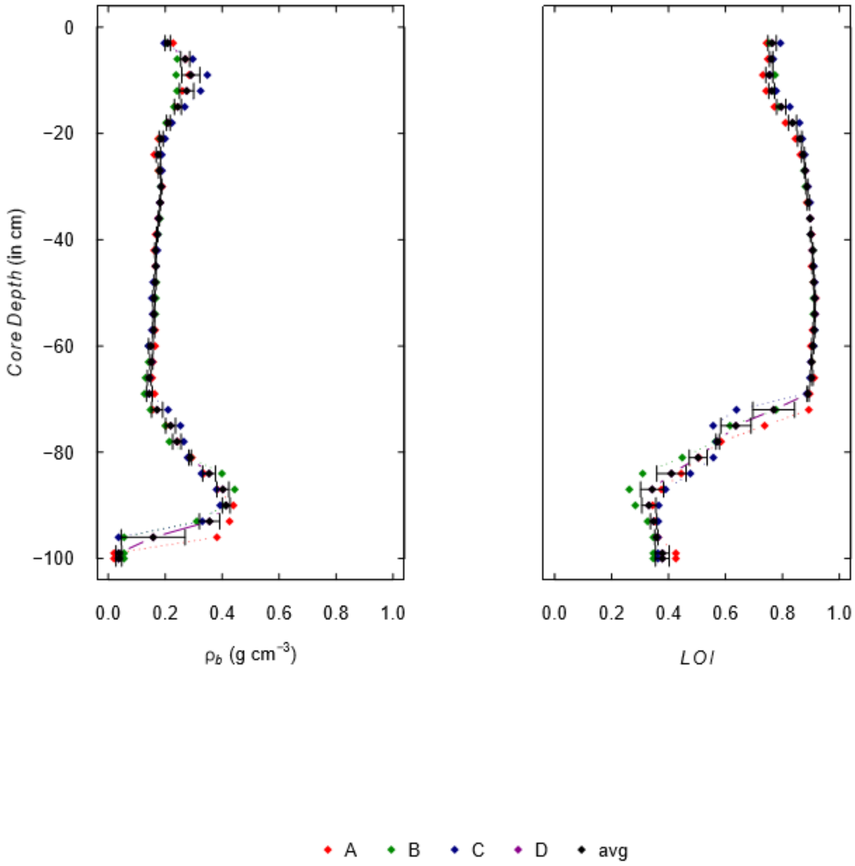

FIGURE 20 Bulk density and Loi at the second site in Germany (N 48°30', E 10°18')

3.1.4 The Netherlands

In FIGURE 21, on the left graph, from 0 cm to 21 cm, the values of bulk density increase sharply and reach the maximum value at 0,72 g/cm^3.while the values decrease vastly to around 0,23 g/cm^3 from 21 cm to 51 cm. From 51 cm to 100 cm, the values change slightly.

On the right graph, from 0 cm to 21 cm, the average of Loi largely decreases from around 0,60 to around 0,40. While the value vastly increases within the range of depth from 21 cm to 48 cm, the average of Loi at 48 cm depth is around 0,83. From 48 cm to 100 cm, the average of Loi almost does not change.

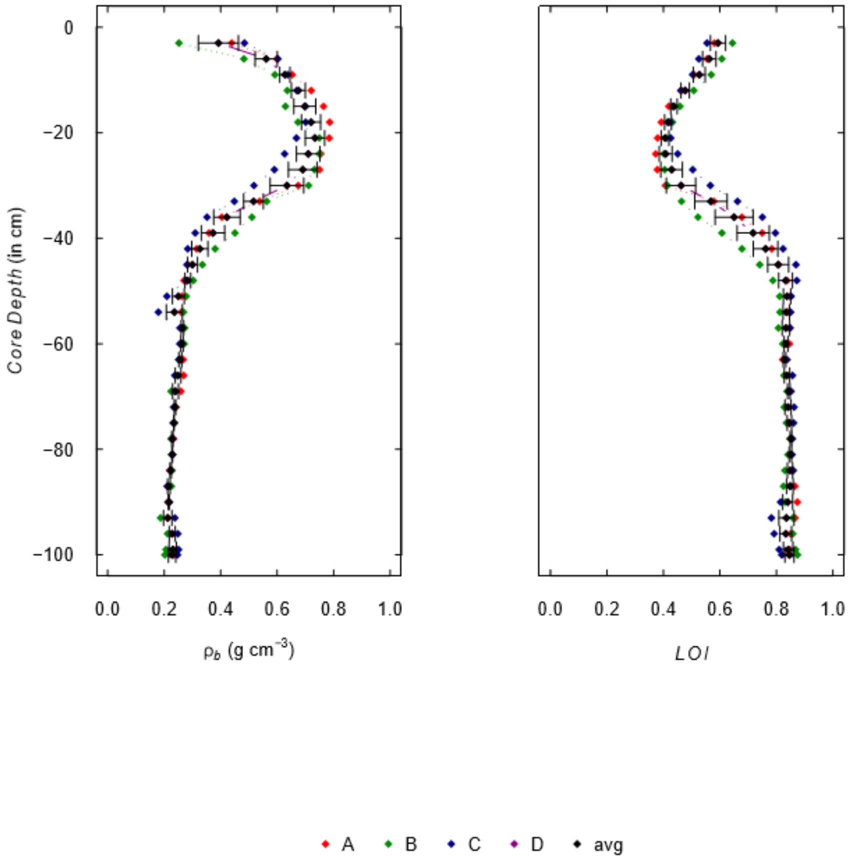

FIGURE 21 Bulk density and Loi at the first site in The Netherlands (N 51°56', E 4°43')

In FIGURE 22, the average of bulk density sharply increases from 0 cm to 12 cm depth, the values increases from around 0, 36 to around 0, 71. From 12 cm to 18 cm, the average of bulk density slightly decreases to around 0, 68. While from 18 cm to 24 cm, the value slightly increases to around 0, 69. From 24 cm to 48 cm, the average value of bulk density sharply decreases to around 0, 26. While from 48 cm to 100 cm depth, the values of bulk density do not have obvious change. On the right graph, from 0 cm to 21 cm, the average of Loi decreases from around 0, 6 to around 0, 42. From 21 cm to 45 cm, the values relatively sharply increase to around 0, 83. However, from 45 cm to 100 cm, the values of Loi are quite homogenous.

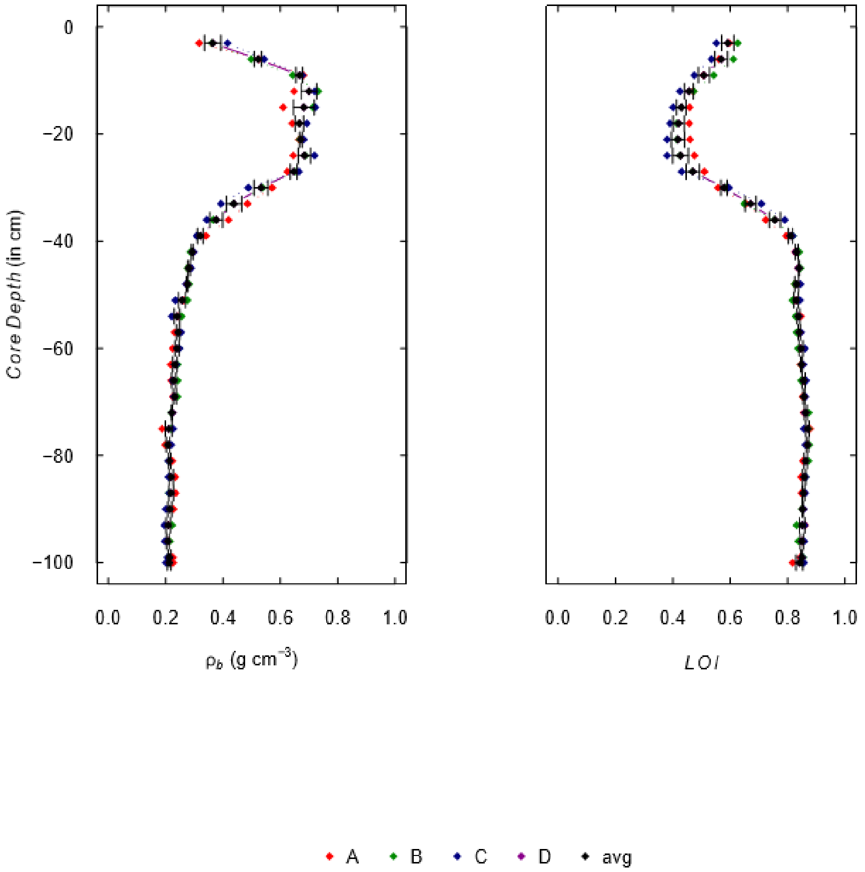

FIGURE 22 Bulk density and Loi at the second site in The Netherlands (N 51°56', E 4°43')

In FIGURE 23, on the left graph, from 0 cm to 18 cm depth, the average value of bulk density sharply increases from around 0,45 g/cm^3 to around 0,86 g/cm^3, which is the maximum value for this soil core sample. While from 18 cm to 57 cm depth, the value sharply decreases to around 0,25 g/cm^3. From 57 cm to 78 cm depth, the average of bulk density almost stays at the same value, while from 78 cm to 87 cm depth, the average of bulk density slightly increases then decreases from 87 cm to 100 cm depth and reaches the lowest value of around 0,22 at 100 cm depth.

On the right graph, from 0 cm to 18 cm, the average value of Loi decreases from around 0,5 to around 0,3. While from 18 cm to 57 cm, the value sharply increases to around 0,79. From 57 cm to 72 cm, the values of Loi almost do not change. From 72 cm to 84 cm depth, the average of Loi slightly decreases to around 0,77 and then increases to 0,89 from 84 cm to 100 cm depth.

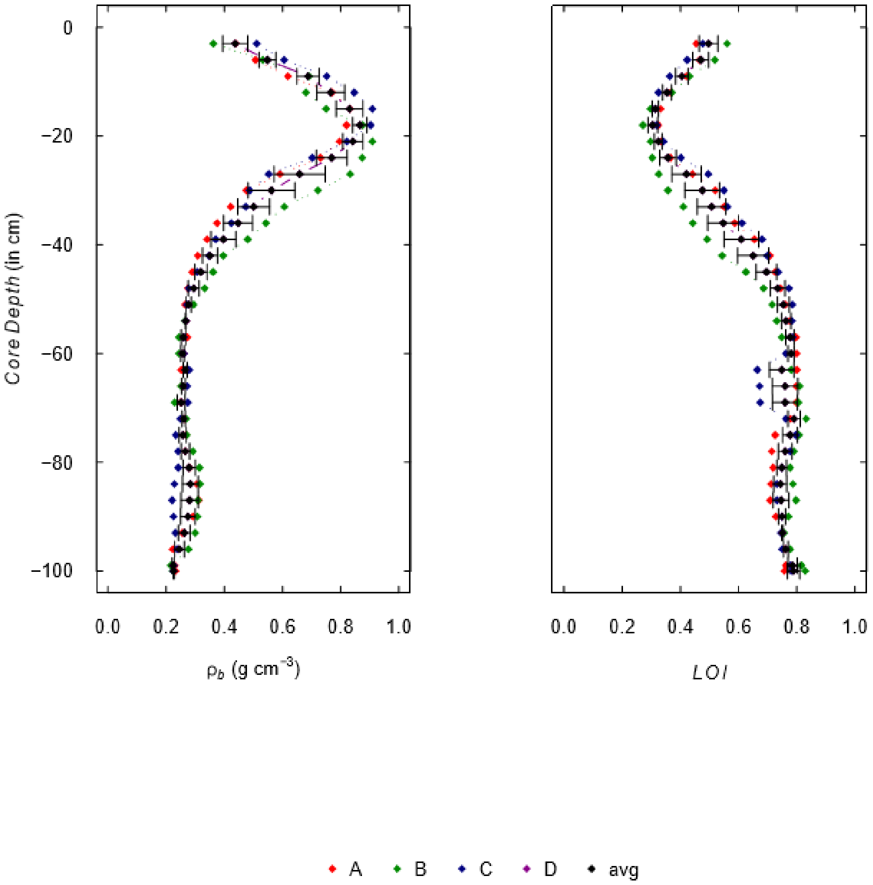

FIGURE 23 Bulk density and Loi at the third site in The Netherlands (N 52°8', E 4°50')

In FIGURE 24, the average value of bulk density sharply increases from around 0,48 g/cm^3 to around 0,90 g/cm^3 from the surface of the ground down to 15 cm depth. However, the average value of bulk density sharply decreases to 0,29 g/cm^3 from 15 cm to 57 cm depth. From 57 cm to 66 cm depth, the average of bulk density almost does not change, while from 66 cm to 75 cm depth, the average of bulk density slightly decreases to around 0,22 g/cm^3. From 75 cm to 87 cm depth, the average of bulk density slightly increases to around 0,27 g/cm^3 and then decreases to around 0,22 g/cm^3 at 100 cm depth.

From the surface of the ground down to 18 cm depth, the average of Loi decreases from around 0,48 to around 0, 31. While from 18 cm down to 51 cm depth, the value increases to around 0,73. From 51 cm 60 cm depth, the average of Loi slightly decreases to around 0,71, then increases to around 7,9 at depth 72 cm. from 72 cm to 81 cm, the average of Loi decreases to around 0,70 and from 81 cm to 87 cm, the average of Loi almost stay at the same value, while from 87 cm to 93 cm, the average of Loi slightly decreases to around 0,67 and then increases to around 0,68 at 100 cm depth.

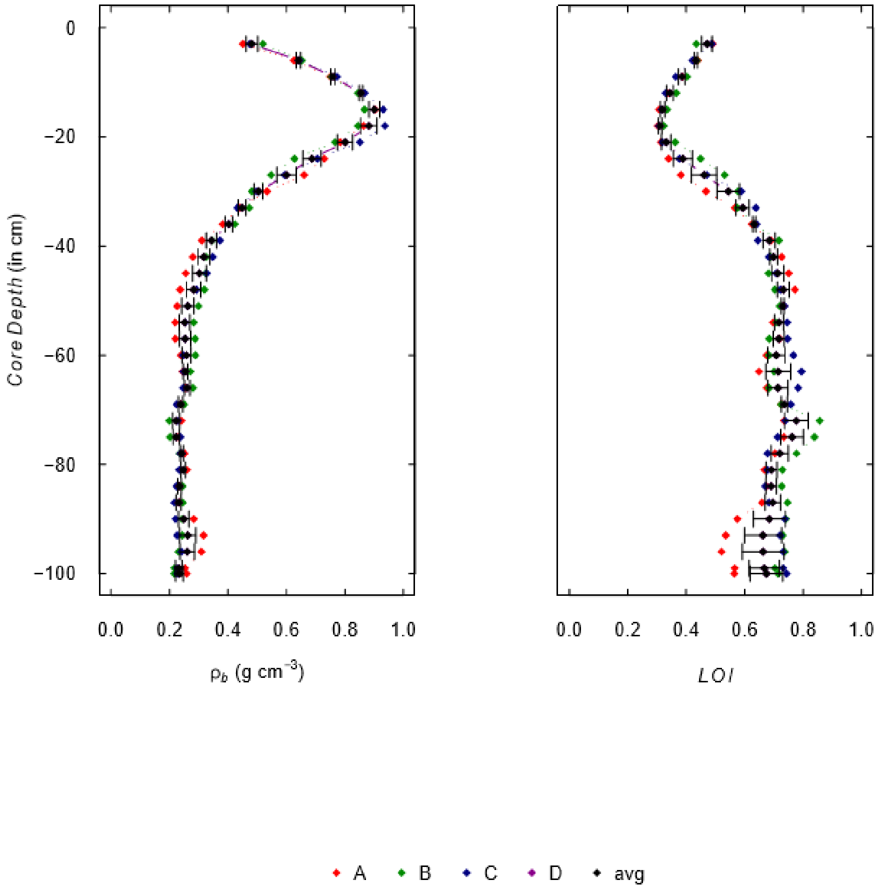

FIGURE 24 Bulk density and Loi at the fourth site in The Netherlands (N 52°8', E 4°50')

3.2 Carbon loss and statistical analysis

3.2.1 Carbon loss in response to land use types

As shown in FIGURE 25, there are seven types of land cover in the studied areas, which are barley, extensively managed grassland (egrass), peat extraction land (extraction), intensively managed grassland (igrass), pasture, paludiculture land (rewetted) and wheat. In all the 15 sites, two of them are rewetted peat lands located in Denmark. There are two extensively managed grasslands located in Denmark as well. There is only one site located on a wheat land in Estonia and one site located on a pasture land in Germany. The intensively managed grasslands are located in Estonia, Germany, and the Netherlands, which are 7 sites in total.

Among all studied land use types, intensively managed grassland has the highest value of carbon loss of approximately 60 kg/m^2. The carbon loss through the wheat land is followed by the second of 33,6 kg/m^2. The pasture land has a carbon loss of 15,4 kg/m^2, while the median value of carbon loss through the two paludiculture land is 13,77 kg/m^2. The two extensively managed grassland in Denmark has a median value of carbon loss with 9,97 kg/m^2. The carbon loss from the barley land and the peat extraction land is measured as 0.

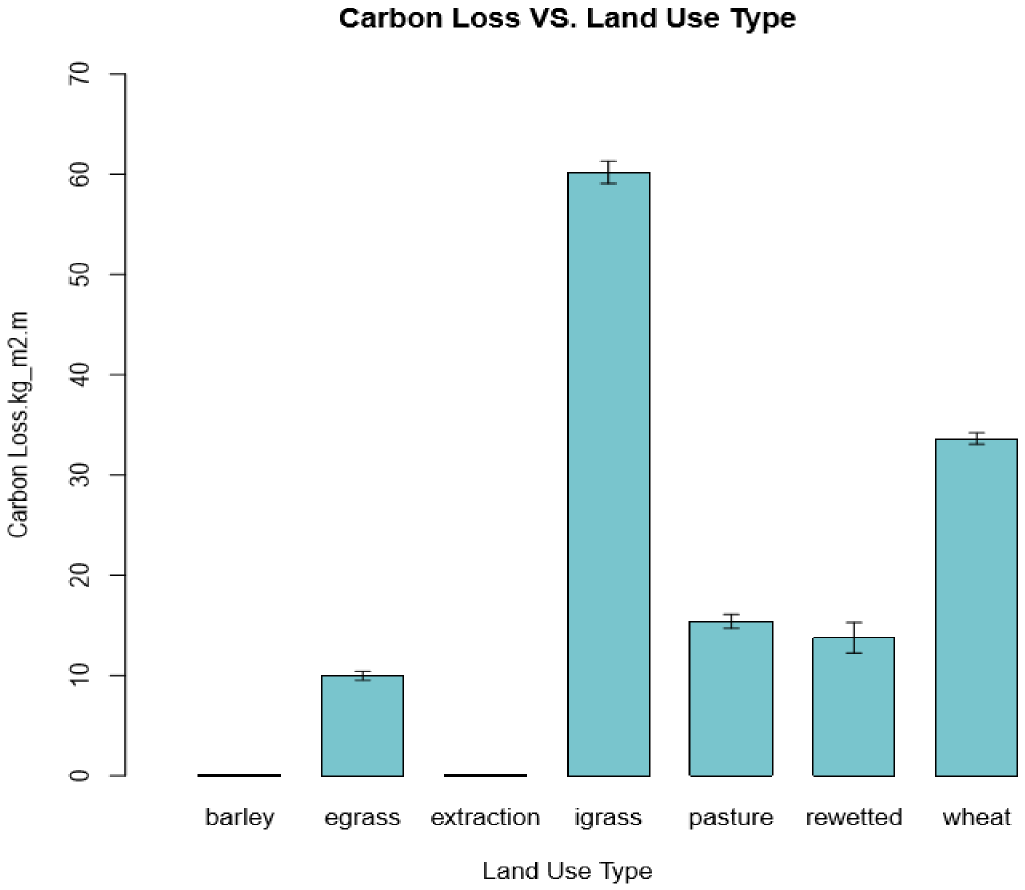

FIGURE 25 Carbon loss associated with land use types

During the statistical analysis, the barley land and wheat land are categorized to arable lands, while the extensively managed grassland, intensively managed grassland, and pasture are categorized to grasslands, while neither the peat extraction land nor the paludiculture land is categorized to each category.

FIGURE 26 indicates the median of carbon loss in unit kilo grams per square meter in response to grassland and arable land types in all studied areas. As shown in the figure, the carbon loss from grassland is approximately 32 kg/m^2, while the value is approximately 17 kg/m^2. Thereby, the values of carbon losses through grassland is almost double compared to arable lands.

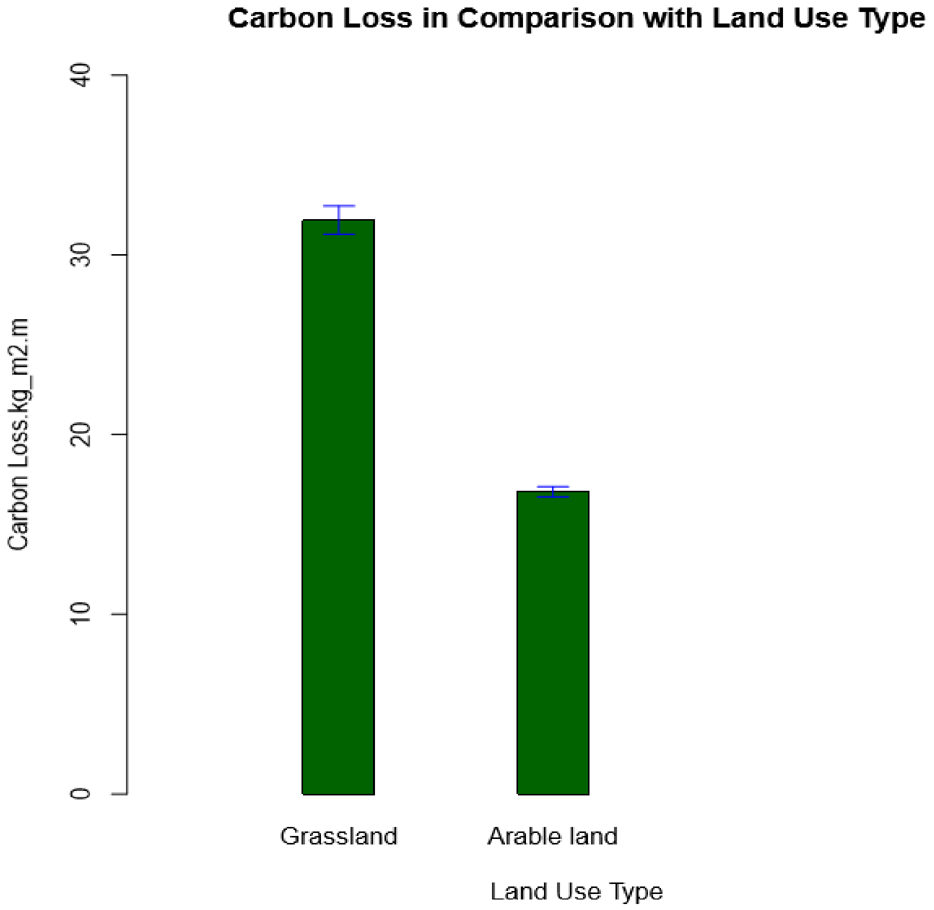

FIGURE 26 Carbon loss associated with lands covered by grass and crops

3.2.2 Carbon loss in response to land use types and cultivation time

The cultivation time is classified into three categories among all sites, which are fewer than 50years, between 50 and 100 years, and more than 100 years. The carbon loss through both grasslands and arable lands are provided in each cultivation time category. As shown in FIGURE 27 below, within the cultivation time range of fewer than 50years, the median value of carbon loss through grasslands is 28,25 kg/m^2, while the value through arable land (barley) is 0. Within the time range between 50 and 100 years of cultivation, the grassland (igrass) has a median carbon loss value of 64,2 kg/m^2, while the arable land (wheat) has a median carbon loss value of 33,64 kg/m^2. Within the time range of cultivation for more than 100 years, the median value of carbon loss through grassland (egrass & pasture) is 15,4 kg/m^2, while the value measured from arable land is 0 due to the land type within this time range of cultivation is not available.

Overall, the median value of carbon loss through grassland is larger than through arable land among all categories of time since cultivation. Wherein, during the cultivation time between 50 and 100 years, the grassland had its highest carbon loss value of 64,2 kg/m^2, while arable land had its highest carbon loss value of 33,64 kg/m^2. However, carbon loss through grassland is almost double of the carbon loss through arable lands. The median value of carbon loss through grassland cultivated for fewer than 50years is 28,25 kg/m^2, while the value is 15,4 kg/m^2 through the grassland cultivated for more than 100 years. The carbon loss through grassland during the cultivation period of fewer than 50years is much lower than through the grassland cultivated between 50 and 100 years, but higher than during the cultivation period of more than 100 years. The carbon loss through grassland within the cultivation period between 50 and 100 years is almost double of the carbon loss through grassland cultivated for fewer than 50 years, which is four times of the value through grassland cultivated for more than 100 years.

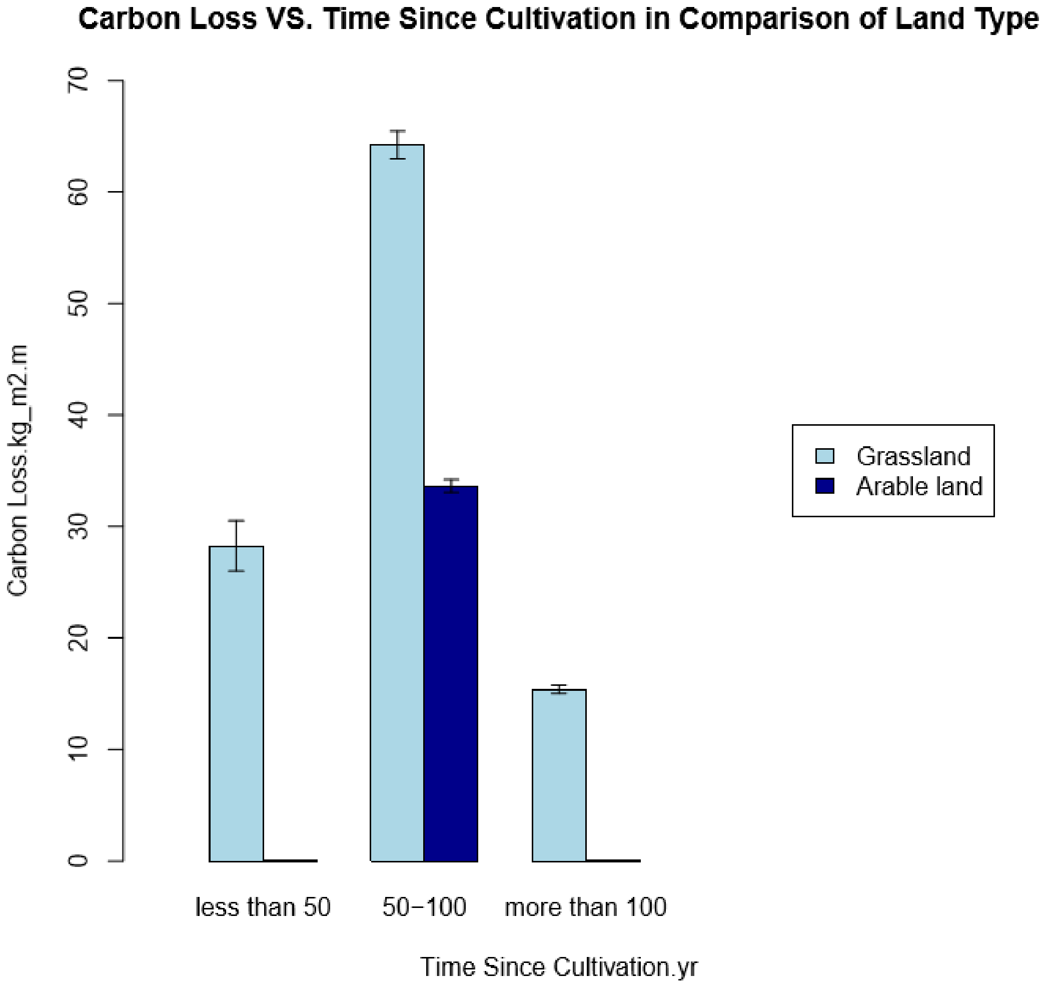

FIGURE 27 Carbon loss associated with cultivation time and land use types

3.2.3 Carbon loss in response to factors influencing the decomposition rate

FIGURE 28 shows the influencing factors of decomposition rate of organic matters in the soil, such as pH-value, the carbon/nitrogen ratio, and the soil temperature. The values of variables are averaged by depth. The extent of decomposition is classified to ten grades, which is from 0 to 10, the larger number refers to stronger decomposition. As shown in the figure. A stronger level of decomposition has a higher carbon loss. The pH-value among all studied sites ranges from approximately 3 to approximately 6, the corresponding values of carbon loss do not change at the range of pH. The C/N ratio among all studied sites mainly stay between 10 and 20, there is only one site has the average C/N ratio of 51,58. The higher C/N ratio, the less carbon loss. The carbon loss tends to increase while the soil temperature increases, the temperature range in all studied sites are from 6 degrees Celsius to 13 degrees Celsius.

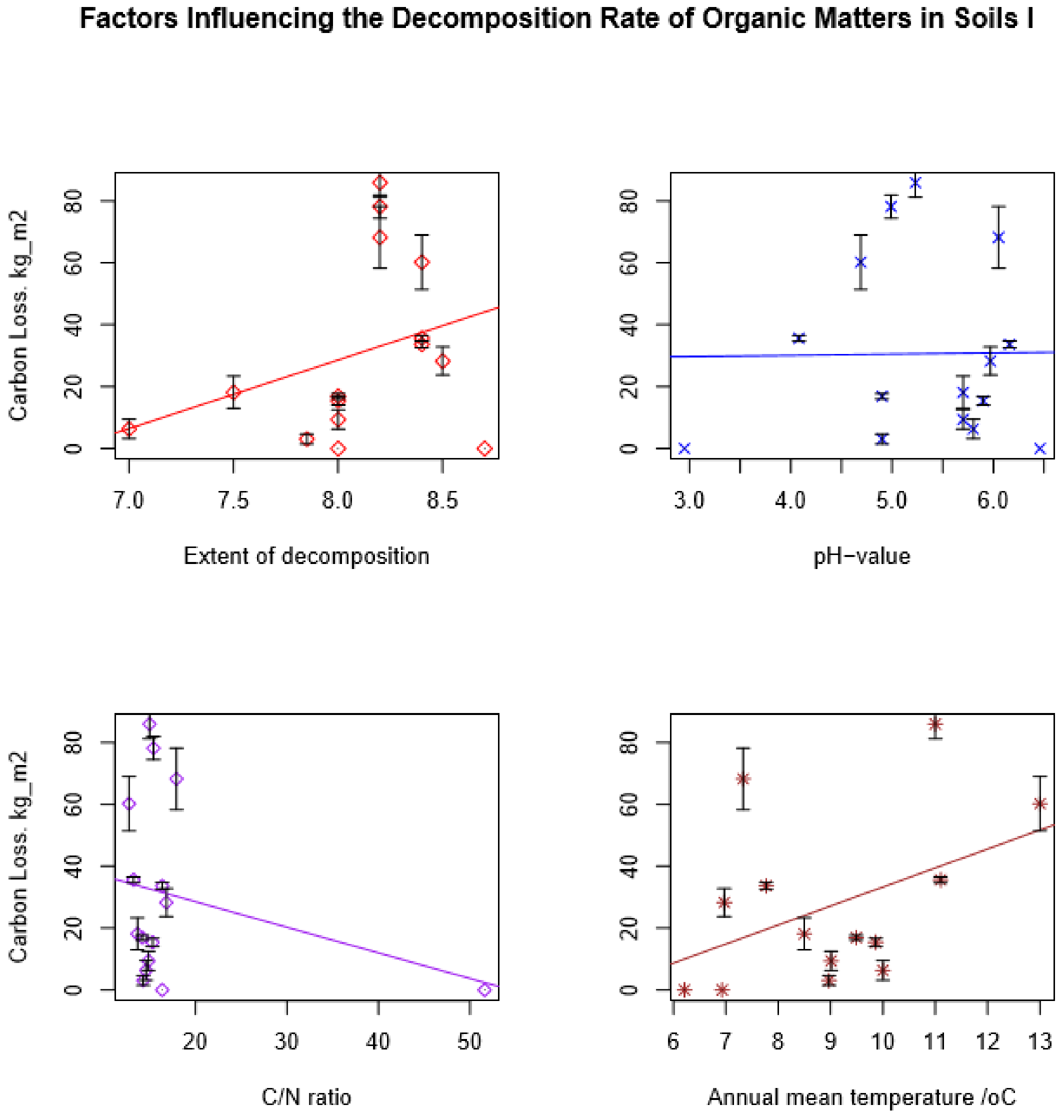

FIGURE 28 Factors influencing decomposing rate in organic soil I

FIGURE 29 shows the factors related to soil moisture affecting carbon loss. There are two types of drainage in all studied sites, one is only with ditches marked with number 1; the other one is with both ditches and pipes underground which is marked with number 2. As shown in the figure below, in general, the mean value of carbon loss through the lands drained by both ditches and pipes is higher than the value of the lands drained by ditches only. The carbon loss tends to decrease while the water table increases in the direction to reach topsoil.

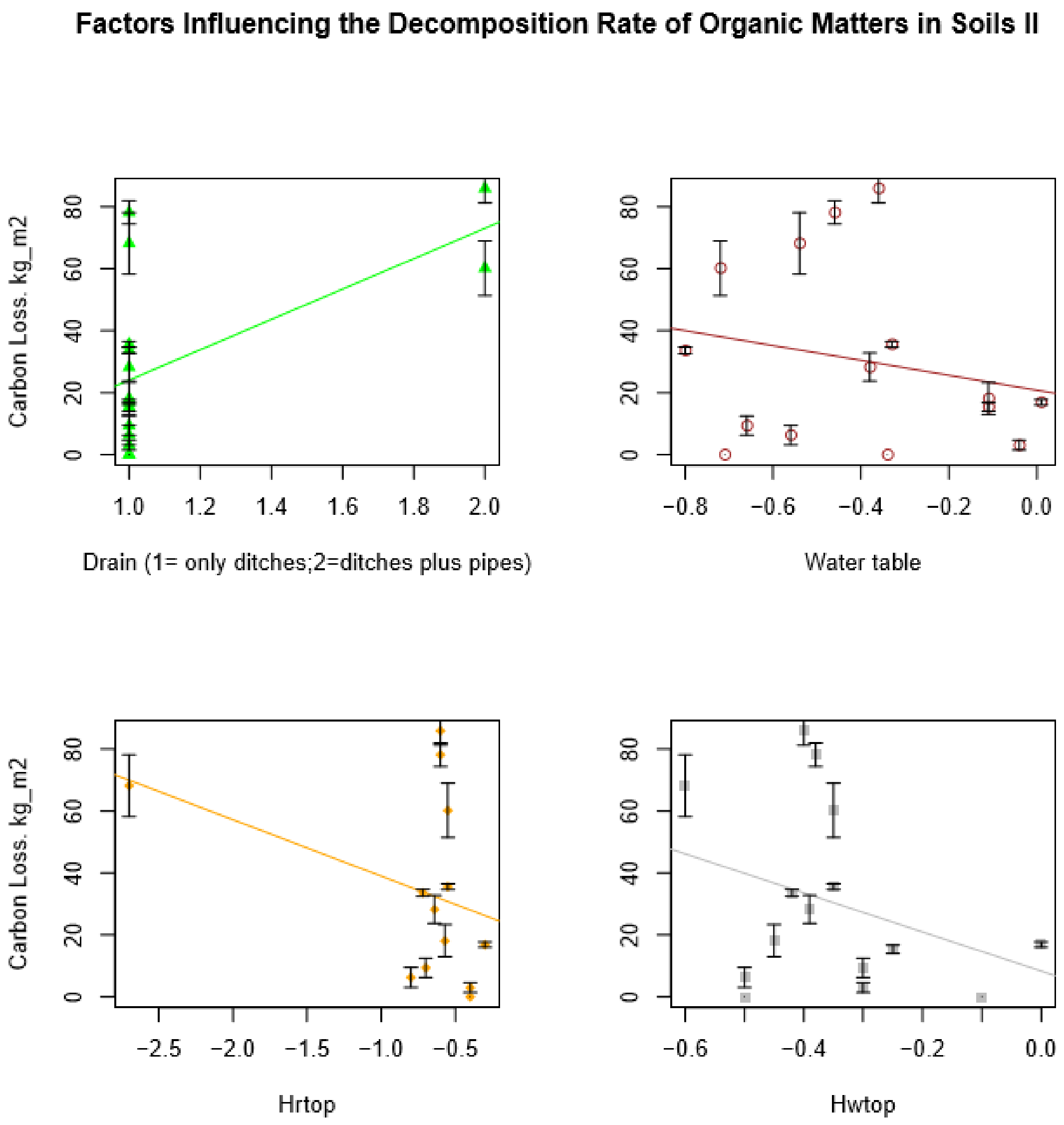

FIGURE 29 Factors influencing decomposition rate in organic soil II

4 DISCUSSION

4.1 Discussion on the bulk density and Loi

Bulk density as one of the physical properties of soil can be used to estimate soil pore space. The organic materials contained in soils can also be estimated according to the trend of bulk density. For instance, among all analyzed soil cores from all studied areas, the bulk density mostly tends to increase first within the depth range between 0 cm and around 15 cm. Then, the bulk density tends to decrease until the depth around 45 cm. however, the bulk density almost does not change from 45 cm depth to 100 cm depth. (USDA. 2008)

However, there are some exceptions such as at the first site and the last site (paludiculture and extensively managed grassland) in Denmark, as well as the two sites (intensively managed grassland and pasture land) in Germany and the fourth site in Estonia (intensively managed grassland), where the bulk density vastly increases from around 75 cm. This is because mineral materials are contained in soils at this range of depth, which has been recognized during the soil preparation in the laboratory. Adding mineral materials, enhance an increase of bulk density, while organic materials enhance a decrease of bulk density.

Changes of bulk density in the 1 m depth of soil core can partially be explained while looking at the value changes of Loi. Overall, the values of Loi at all studied sites decrease first from the topsoil downward to around 15 cm to 21 cm depth, indicating at this range of depth that the organic content is decreasing. Then, from the depth range of 15 cm ~ 21 cm to the depth of around 45 cm, the values of Loi increase due to the increasing organic content in soils. Continuing from 45 cm depth, the Loi has the same situation as bulk density, which stays at relatively stable values, which indicates at this range of depth, the organic materials content stays at a relatively high and stable value. However, at some sites, the values of Loi greatly decrease from around 45 cm depth, this might because the appearance of rocks or clay in the subsoil.

Continuing from the soil surface to the depth of around 15 cm to 21 cm, the bulk density largely increases. Meanwhile, the Loi decreases. However, the decreasing rate of Loi is slower than the increasing rate of bulk density, indicating organic matters are reducing. (USDA. 2008)

4.2 Discussion on land use types influencing the carbon loss

As shown in the statistical data, grasslands have more carbon loss than arable lands. One of the leading reasons is the level of carbon pristine contained. In general, the studied grasslands have more pristine carbon than the arable land. When the number of the elementary set is larger, it is reasonable to have a larger output as well. Hence, the more organic carbon is contained, the more carbon is lost. As shown in FIGURE 25, intensively managed grassland has the highest value of carbon loss among all studied land cover types. The median value of the pristine carbon content in intensively managed grassland is the largest value at all studied sites. Due to the current data could not support the hypothesis, the other factors affecting soil conditions, such as temperature, water table, carbon/nitrogen ratio, drainage type and so forth, should be analyzed.

4.3 Discussion on factors influencing the decomposition rate of organic matters

As expected from the hypothesis for this work, the arable lands are supposed to have a higher carbon loss than grassland. However, according to the obtained data as shown in FIGURE 26, the results are contrary to the expectations, in which the grassland has a much higher carbon loss than arable land. In addition, as shown in FIGURE 27, the land with a cultivation time between 50 and 100 years has the highest carbon loss value; carbon loss from lands cultivated for fewer than 50years has the second highest carbon loss. The carbon loss from lands cultivated for more than 100 years has the lowest value. As shown in FIGURE 28, the carbon loss through grassland is always higher than through arable land in all cultivation time categories.

Therefore, the acquired results may correlate with other factors influencing carbon loss from organic soils that the variables affecting decomposition, drainage types and soil chemical properties such as C: N ratio and pH-values. Therefore, a statistical analysis of carbon loss associated with all these factors is conducted.

As shown in FIGURE 28, high level of decomposition correlates with a higher value of carbon loss. Soil pH is a significant factor for the decomposition of organic materials in the soil. A low pH value is a sign of an acidic condition of the soil, while a high pH value causes an alkaline soil environment. However, neither too low nor too high pH levels are beneficial for microbial activity. The microbes tend to be more active regarding decomposition of organic matters in the neutral or slightly alkaline soils in pH than acidic soils. The decomposition rate could sharply decrease while the pH-value is under 6 (The Ohio State University. 2010). As shown in FIGURE 28, in general, the pH values at sites are below 6, the carbon loss does not change along with pH changes.

Microbes and microorganisms are more in favor of a warm temperature for decomposition of organic matter; usually, a temperature between 25 and 30 degrees Celsius is optimum for decomposition. The reproduction rate of microbes is double while the temperature increases every 10 F. Microbes decompose much quicker in warm conditions than in colder conditions. The temperature ranges from 6 degrees Celsius to 13 degrees Celsius, which does not reach the optimum temperature for decomposition, however, an increase of carbon loss along with temperature rises is indicated. The annual mean temperature at sites in The Netherlands is apparently higher than the other sites, which might lead to more carbon loss through intensively managed grassland. (The Ohio State University. 2010)

The oxygen is the compulsory condition for aerobic decomposition that producing CO_2. The loose soils and those soils whose pores are not filled up with water are more likely to be able to access oxygen. Soil types such as clay are too tight to provide conditions for decomposition. Processes enhancing high oxygen levels in the soil can accelerate the decomposition rate, thereby increasing the production of CO_2. The possible processes could be cultivation and drainage. (Agriinfo. 2015)

The water content in soils can, directly and indirectly, influence the microbial activity in soils. A high water content in the soil can slow down the decomposition rate, as the soil pores are filled up with water, causing oxygen to be unavailable for the decomposition process. Meanwhile, water can also dissolve CO_2 into carbonic acid, which decreases the possibility of releasing CO_2 through soils into the atmosphere. The drainage type with ditches and manual pipes is more efficient than the type that only uses ditches, which enhances oxygen that is constantly available in soil pores and thus producing and accumulating more CO_2.

However, if there is too little water contained in soils, the soil would turn very dry, which is threatening the survival of microbes. Therefore, an appropriate and constantly humid condition in soils enhance a quick decomposition rate. (The Ohio State University. 2010)

Carbon and nitrogen are the food factors affecting decomposing processes by bacteria, fungi, and microorganisms. Wherein carbon is used as an energy source for bacteria to consume, nitrogen is used as protein for bacteria to grow and reproduce more bacteria. In different organic matters, the carbon/nitrogen content is different. The condition with higher nitrogen content helps microbes decompose faster. Generally, about two-thirds of carbon is respired as CO_2 in soils, while the other third is combined with nitrogen in the living cells. However, if the excess of carbon over nitrogen (C:N ratio) in organic materials being decomposed is too great, biological activity diminishes. Several cycles of organisms are then required to burn most of the carbon. (Agriinfo. 2015)

To analyze whether above-mentioned variables have an impact on the level of carbon loss or not, the values of all factors are compared. It has been recognized that the soil temperature at sites in intensively managed grasslands cultivated for 50 to 100 years is generally higher than the other sites. The median of the ground water table at sites from grasslands cultivated for more than 100 years is the highest, which is -0,04 m. The median value of ground water table in grasslands cultivated for more than 100 years is the second highest, which is -0,38 m. While the grasslands cultivated for 50 to 100 years have the lowest water table that is -0,41 m. This indicates warmer temperature and lower water table due to drainage could accelerate the decomposition rate and carbon loss from soil.

4.4 Recommendations

Expanding the study areas in order to make sure the number of sites from all different land types is equal or large enough. This is crucial in order to find out the median value. For instance, the number of sites from paludiculture lands and extensively managed grassland are even, which are two sites, therefore, the calculation of the median value of the two sites is equal to calculate the mean. However, while conducting a statistical analysis of the influence of cultivation time on carbon loss, there are three sites that belong to the cultivation time with fewer than 50years. The carbon loss values of the three sites are 0; 28,25 kg/m^2; 0, hence the median value of carbon loss within this range of cultivation time is 0 instead of 9,42 kg/m^2 (the mean value).

Moreover, there are only two sites in the category of arable land, which are: wheat and barley. The wheat land has a cultivation time of 52 years which is classified to the cultivation time category "between 50 and 100 years". Barley land has a cultivation time of 41 years which is classified to the category "fewer than 50years". However, the data from arable lands in category "more than 100 years" is not available, which has limited the data range. For a certain cultivation time category, the size of the database is various, the data representative possibility is questionable while the size of the database is too small. For instance, there is only one site from wheat lands studied among three cultivation time categories.

In addition, while studying the influence of cultivation time on carbon loss, the obtained results show not necessarily longer cultivation time leads to a higher value of carbon loss. However, the land cover types are not consistent among all cultivation time categories, in the category of "fewer than 50years", the size of database is three and from three different land cover types, which are: extracted peat land, intensively managed grassland, and barley land, however, the carbon loss from two sites (extracted peat land and barley land) is measured as zero, therefore, only the data from intensively managed grassland is effective. While looking for the median of carbon loss in this cultivation time category, the other two zero values are included, which lead to a zero value of carbon loss in this time category. Significant data is missing in this category, therefore, samples from arable lands cultivated for fewer than 50years should be taken for further analysis.

In the time since cultivation category of "more than 100 years", five sites including three land cover types are covered, which are two paludiculture peat lands, two extensively managed grasslands, and one pasture land. Differing from the land cover types in the above two cultivation time categories, the time category "between 50 and 100 years" covers seven sites including two land cover types, which are six sites of intensively managed grassland and one wheat land. The lengths of data in the three categories of time since cultivation are different from each other, data is missing from arable lands in some category, which brought a difficulty to compare and summarize and lead to the current statistical results might not be representative.

5 CONCLUSIONS

Soils high in pristine carbon content show more of carbon losses than soils low in pristine carbon content. Intensively managed grassland has the highest pristine carbon level, which has the highest median value of carbon loss at all sites as well. The carbon loss at sites decreases in the following order: igrass > wheat > pasture > paludiculture land > egrass. The carbon loss/pristine carbon ratio decreases in the following order: igrass > wheat > pasture > egrass> rewetted peat land. If excluding the zero values of carbon loss which are barley and peat extraction land, as well as the rewetted peat land, the carbon loss decreases in the following order: Arable land > grassland. Where arable land refers to the site wheat, and grasslands refers to igrass, pasture, and egrass lands. Therefore, manmade activities such as cultivation of lands induce the carbon loss through soils to the atmosphere, affect global climate change and cause global warming. Further conclusions based on the impact of cultivation and drainage on the carbon loss are difficult to be drawn due to the current small databases.

A comprehensive summary of the factor of cultivation time affecting carbon loss is quite challenging in this work due to the limit of the database. Longer cultivation time causes more carbon loss can be seen while comparing the median value of carbon loss through intensively managed grassland in both “fewer than 50years” and “between 50 and 100 years” categories; the latter has a higher value of carbon loss than the former.

The most decomposed organic materials concentrate in the topsoil. Optimum soil conditions accelerate the decomposition rate, thus cause more carbon dioxide being released into the atmosphere. In general, parameters such as the extent of decomposition and soil temperature are proportional to the values of carbon loss, while parameters such as C/N ratio and water table are inversely proportional to the values of carbon loss. The pH value under 6 does not show a significant influence on levels of carbon loss. A higher water table lowers the oxygen level in soils, thus slowing down the microbial decomposition rate of organic matters, which leads to a lower value of carbon loss. Drainage with ditches and manual pipes indicates a higher level of carbon loss than the drainage which only occurs in ditches. Therefore, agriculturally efficient drainage may induce carbon emissions through soils to the atmosphere, thus causing global warming as well.

REFERENCES

Agriinfo. (2015). Factors Influencing rate of Organic Matter Decomposition. Read 24.1.2018. http://agriinfo.in/default.aspx?page=topic&superid=7&topicid=170

A.Piayda. (2017). Communication in person.

B. Tiemeyer. (2017). Documental pictures of soil core sampling.

Climate-data. org. CLIMATE: GÜNZBURG. Read 14.1.2018. https://en.climate-data.org/location/19365/

D. Schimel, I.G.Enting, M. Heimann, T.M.L.Wigley, D.Raynaud, D.Alves, U.Siegenthaler. (2000). CO_2 and the Carbon Cycle. The Carbon Cycle. Extracted from “Climate Change, 1994”, Intergovernmental Panel on Climate Change (IPCC) Report. p8.

EPA. (2017). Total greenhouse gas emission trends and projections. Read 8.1.2018. https://www.eea.europa.eu/data-and-maps/indicators/greenhouse-gas-emission-trends-6/assessment-1

European commission. Eurostat. Land cover/use statistics (LUCAS). Read 5.1.2018. http://ec.europa.eu/eurostat/web/lucas

Eurostat. (2016). File:Greenhouse gas emissions, EU-28, 2012.png. Read 10.1.2018. http://ec.europa.eu/eurostat/statistics-explained/index.php/File:Green-house_gas_emissions,_EU-28,_2012.png

GEOLAB. (2016). Window sampling set. Read 11.1.2018. http://geolab.com.pl/files/Oferta/02_Grunty_sprzet_terenowy/08_Sonda_rdzeniowa_RKS/Window_sampling_set_RKS.pdf

IPCC. (2014). Climate Change 2014: Mitigation of Climate Change. Read 8.1.2018. https://www.ipcc.ch/report/ar5/wg3/

IPCC. AR5, Chapter 11. Read 10.1.2018. https://www.ipcc.ch/pdf/assessment-report/ar5/wg3/ipcc_wg3_ar5_chapter11.pdf

J. P. Krüger, J. Leifel, S. Glatzel, S. Szidat, C. Alewell. (2015). Biogeochemical indicators of peatland degradation – a case study of a temperate bog in northern Germny. Biogeosciences, 12, 2861 – 2871, 2015. www.biogeosciences.net/12/2861/2015/

J.T.Houghton, Y.Ding, D.J.Griggs, M.Noguer, P.J.van der Linden, X.Dai, K.Maskell, C.A.Johnson. (2001). Climate Change 2001: The Scientific Basis. Intergovernmental Panel on Climate Change. CAMBRIDGE UNIVERSITY PRESS. P6.

M.J.J.Hoogsteen, E.A.Lantinga, E.J.Bakker, J.C.J.Groot, P.A.Tittonell. (2015). Estimating soil organic carbon through loss of ignition: effects of ignition conditions and structural water loss. Eur J Soil Sci, 66: 320–328. doi:10.1111/ejss.12224

NASA. (2017). Carbon Dioxide. GLOBAL CLIMATE CHANGE. Read 2.1.2017.

https://climate.nasa.gov/vital-signs/carbon-dioxide/

NASA. (2007). How is Today's Warming Different from the Past?. Read 14.1.2018. https://Earthobservatory.nasa.gov/Features/GlobalWarming/page3.php

National Oceanic and Atmospheric Administration (NOAA). Carbon Cycle Science. U.S. Department of Commerce. U.S. Department of Commerce. Read 2.1.2018. https://www.esrl.noaa.gov/research/themes/carbon/

R. Lindsey. (2009). Climate and Earth's Energy Budget. The Earth Observatory. Read 25.12.2017. https://Earthobservatory.nasa.gov/Features/EnergyBalance/page4.php

S. Trumbore, O. Chadwick, R. Amundson, B. Brasher. (1994). Effect of Climate on the Storage and Turnover of Carbon in Soils. Final Technical Report for NASA- NAG 5 1840. ASA-CR-I96278.

The R Foundation. (2017). The R Foundation for Statistical Computing. Read 28.11.2017. https://www.r-project.org/

The World Bank. 2014. Average precipitation in depth (mm per year). Read 14.1.2018. https://data.worldbank.org/indicator/AG.LND.PRCP.MM

The Ohio State University. (2010). UNDERSTANDING SOIL MICROBES AND NUT RIENT RECYCLING. Agriculture and natural resources. SAG-16. Read 18.1.2018. https://ohioline.osu.edu/factsheet/SAG-16

Tutorialspoint. R tutorial. Read 6.11.2017. https://www.tutorialspoint.com/r/index.htm

USDA. (2014). United States Department of Agriculture. Soil physical and chemical properties. Physical properties. Bulk density. Read 15.1.2018. https://www.nrcs.usda.gov/wps/portal/nrcs/detail/nj/home/?cid=nrcs141p2_018993#Bulk_Density_

USDA. (2008). United States Department of Agriculture. Soil Quality Indicators. Bulk density. Read 24.1.2018. https://www.nrcs.usda.gov/Internet/FSE_DOCUMENTS/nrcs142p2_053256.pdf

UNH. (2009). The University of New Hampshire. An introduction to the global carbon cy cle.GLOBE Carbon Cycle. Read 5.9.2017. http://globecarboncycle.unh.edu/CarbonCycleBackground.pdf

UNH. (2008). The University of New Hampshire. Durham, NH 03824. Read 2.1.2018. http://globecarboncycle.unh.edu/CarbonPoolsFluxes.shtml

V. Walt. (2014). Window Sampling and the Percussion Drilling Rig. 11.1.2018. https://www.youtube.com/watch?v=t_VZxXHNF_k

Yu, Z., Beilman, D. W., Frolking, S., MacDonald, G. M., Roulet, N.T., Camil, P., and Charman, D. J. (2011). Peatlands and Their Role in the Global Carbon Cycle, EOS, 92, 97-106.

APPENDICES

Appendix 1. Table of compiled data for statistical plots

Site	C.kg_m^2_sem	C.kg_m^2	CLoss.kg_m^2_sem	CLoss.kg_m^2	CPristine.kg_m^2_sem	CPristine.kg_m^2	S.m_sem	S.m	Sp.m_sem	Sp.m	Ss.m_sem	Ss.m	Analysed_Depth.m	Cultivation_time	Use_type
DK01	6.994.499	8.468.338	51.934.910	18.136.339	18.010.080	10.281.972	0.06233757	0.32596166	1,10E+03	1,49E+05	0.063434813	0.17687555	0.66	more than 100	rewetted
DK02	5.925.716	8.286.904	30.808.615	9.386.867	28.448.541	9.225.591	0.03364266	0.13047183	8,29E+02	4,20E+04	0.034472112	0.08846077	0.72	more than 100	rewetted
DK04	2.445.077	5.313.376	0.8180801	16.902.552	31.658.933	7.003.631	0.02178245	0.36806961	1,53E+04	1,58E+05	0.008024451	0.20991051	0.51	more than 100	egrass
DK05	1.790.918	7.636.698	15.828.630	3.030.512	36.840.324	7.883.553	0.03836259	0.09031638	1,57E+04	6,33E+04	0.017752225	0.03330038	0.78	more than 100	egrass
EE01	4.326.859	7.678.745	0.0000000	0.000000	48.696.425	7.505.585	0.00000000	0.00000000	1,84E-11	3,47E-11	0.000000000	0.00000000	0.96	0	extraction
EE04	3.719.977	10.949.971	99.550.357	68.209.152	122.925.346	17.770.887	0.06197827	0.64369693	1,93E+04	6,06E+04	0.069844440	0.58309921	0.90	52	igrass
EE05	1.530.474	10.857.596	11.388.303	33.638.033	0.4940672	14.221.400	0.00612384	0.40972255	7,19E+03	8,79E+04	0.013286832	0.32185117	0.96	52	wheat
EE06	5.925.017	10.774.808	45.278.778	28.252.402	69.777.101	13.600.048	0.03763682	0.53850541	7,37E+03	2,73E+05	0.043521890	0.26508377	0.75	41	igrass
EE07	1.243.961	12.778.205	0.0000000	0.000000	15.003.661	12.588.157	0.00000000	0.00000000	1,31E-11	2,43E-11	0.000000000	0.00000000	0.87	41	barley
DO01	6.946.970	10.640.437	31.620.794	6.323.862	32.652.589	11.200.609	0.04388539	0.10110826	2,08E+04	5,29E+04	0.026718781	0.05316332	0.78	50-100	igrass
DO03	1.255.860	5.699.229	13.721.657	15.398.912	13.747.055	7.239.120	0.01339423	0.25913933	1,50E+04	5,80E+04	0.017291454	0.20111829	0.69	more than 100	pasture
NLS01	1.829.914	11.176.660	46.886.855	85.916.675	48.308.145	19.768.328	0.05852148	102.503.050	7,34E+03	2,29E+05	0.051204952	0.79598932	0.87	50-100	igrass
NLS02	1.476.005	11.370.563	37.575.846	78.165.490	24.672.127	19.187.112	0.03240074	0.96035701	7,24E+03	2,14E+05	0.039299408	0.74684144	0.93	50-100	igrass
NLS03	3.013.848	8.482.699	87.851.210	60.195.974	61.015.296	14.502.296	0.07850988	0.79543508	2,51E+04	1,97E+05	0.092511857	0.59862730	0.72	50-100	igrass
NLS04	2.595.676	9.228.673	0.9292252	35.608.577	30.033.135	12.789.531	0.02528824	0.58676928	1,30E+04	2,28E+05	0.013446544	0.35884929	0.78	50-100	igrass

Appendix 2. The geographical locations and the description of sites

Site	Lattitude	Longitude	Drainage type	Drainage time/yr	Cultivation time/yr	Land type/cover	Address
DK01	56.45903725	9.678085644	1	100	more than 100	Rewetted peatland	stervangsvej 93, 8830 Tjele, Denmark
DK02	56.45772136	9.675710845	1	100	more than 100	Rewetted peatland	stervangsvej 93, 8830 Tjele, Denmark
DK04	56.49215617	9.863007964	1	100	more than 100	Extensively managed grassland	Viborgvej 370, 8920 Randers NV, Denmark
DK05	56.49275479	9.862538847	1	100	more than 100	Extensively managed grassland	Viborgvej 370, 8920 Randers NV, Denmark
EE01	58.51518022	27.01071651	unknown	unknown	0	Extracted peatland	Lauka, Sookalduse, 60421 Tartu maakond, Estonia
EE04	58.25935146	26.1507742	1	0	52	Intensively managed grassland	Hällimäe tee 9, Tamme, 61114 Tartu maakond, Estonia
EE05	58.25919332	26.15254121	1	0	52	Wheat	Hällimäe tee 9, Tamme, 61114 Tartu maakond, Estonia
EE06	58.2199211	26.29200525	1	0	41	Intensively managed grassland	Kraavi, Konguta, 61217 Tartu maakond, Estonia
EE07	58.21971604	26.29138439	1	0	41	Barley	Kraavi, Konguta, 61217 Tartu maakond, Estonia
DO01	48.50248572	10.25982775	1	50	50-100	Intensively managed grassland	89312 Günzburg, Deutschland
DO03	48.50960335	10.30093476	1	100	more than 100	Pasture	Unnamed Road, 89423 Gundelfingen an der Donau, Germany
NLS01	51.94871	4.723471	2	0	50-100	Intensively managed grassland	Benedenheulseweg 37, 2821 LV Stolwijk, Netherlands
NLS02	51.947951	4.723769	1	100	50-100	Intensively managed grassland	Benedenheulseweg 37, 2821 LV Stolwijk, Netherlands
NLS03	52.138306	4.840885	2	0	50-100	Intensively managed grassland	Oude Meije 16, 3474 KM Zegveld, Netherlands
NLS04	52.139021	4.8409	1	50	50-100	Intensively managed grassland	Oude Meije 16, 3474 KM Zegveld, Netherlands

* 1 refers to only with ditches, 2 refers to with ditches and pipes

(Source: J.T.Houghton, Y.Ding, D.J.Griggs, M.Noguer, P.J.van der Linden, X.Dai, K.Maskell, C.A.Johnson. 2001)

Indicators of the human influence on the atmosphere during the Industrial Era

(a) Global atmospheric concentrations of three well mixed greenhouse gases

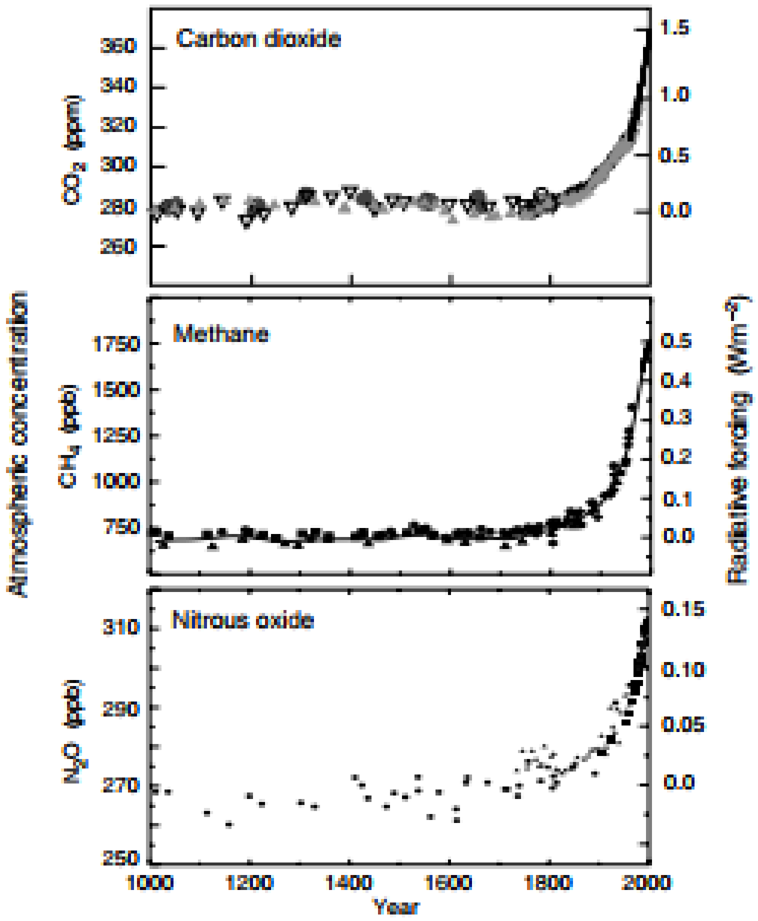

(b) Sulphate aerosols deposited in Greenland ice

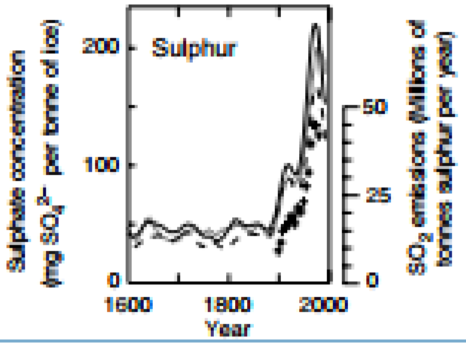

Appendix 4. Trends, estimation, and targets of GHGs in the EU, 1990-2050

(Sources: EEA, 2017a,2017b,2017c,2017d)

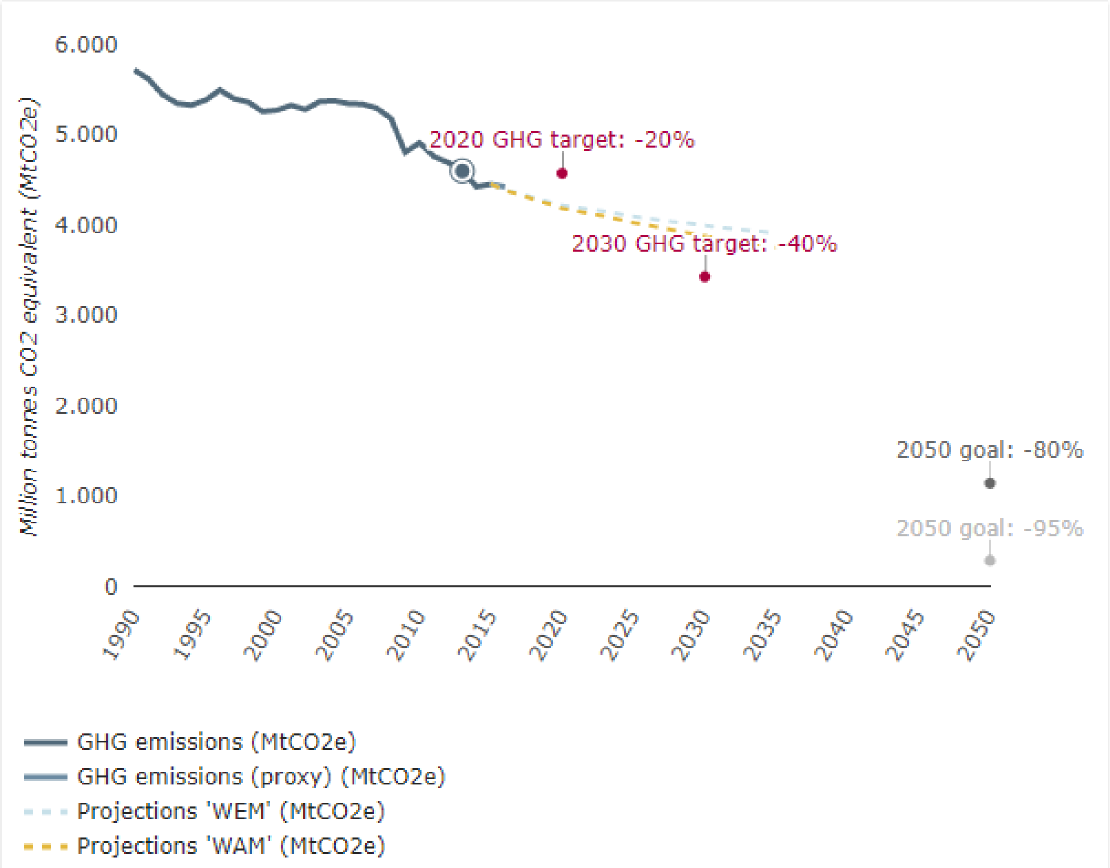

Note:

The GHG emission trends, projections and targets include emissions from international aviation, and exclude emissions and removals from the land-use sector (LULUCF). For greenhouse gas (GHG) projections, the 'with existing measures' (WEM) scenario reflects existing policies and measures, while the 'with additional measures' (WAM) takes into account the additional effects of planned measures reported by Member States. These projections were reported in 2017.

Appendix 5. A comparison of GWP

(Source: IPCC AR4)

Different greenhouse gases have different contributions to global warming. Using the global warming potential (GWP) of CO_2 as a base, before 2015, the GWP of CH_4 is 21 times of CO_2 meaning for instance 1 tonne of CH_4 can cause the same warming as 21 tonnes of CO_2. N_2O has a 310 times of GWP over CO_2, while F-gases have 23,900 times higher global warming potential than CO_2. Global warming potential (GWP) is an approach to assess to what extent the greenhouse gases can contribute to global warming on a 100-year horizon. (EPA. 2017)

Gas	GWP [before 2015]	GWP [after 2015]
Carbon dioxide (CO2)	1	1
Methane (CH4)	21	25
Nitrous oxide (N2O)	310	298
Sulphur hexafluoride (SF6)	23900	22800
Nitrogen trifluoride (NF3)	_	17200

(Source: IPCC. 2014)

By gas

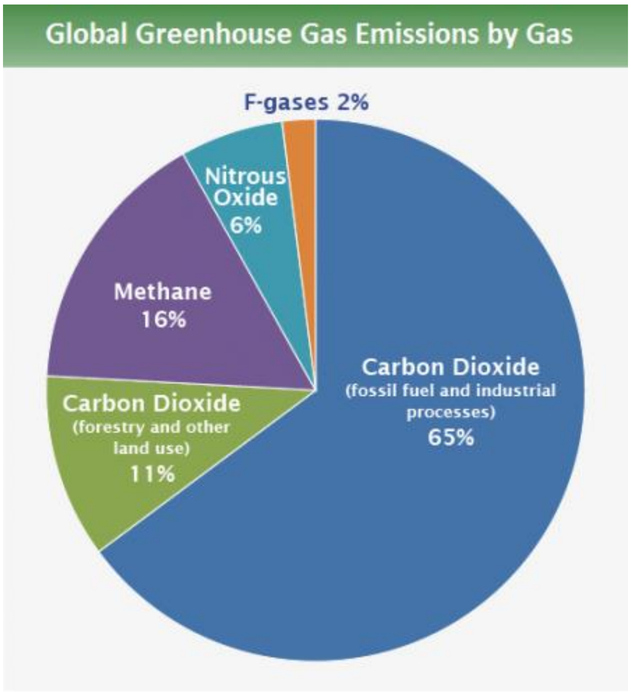

By primary region and countries

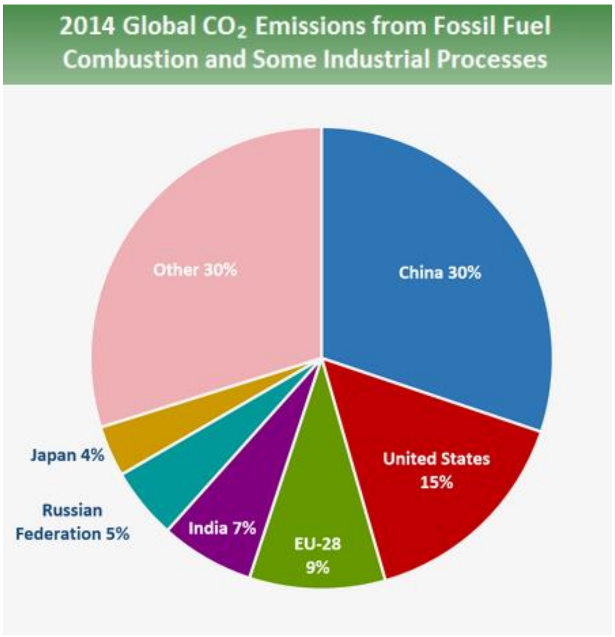

By source sector

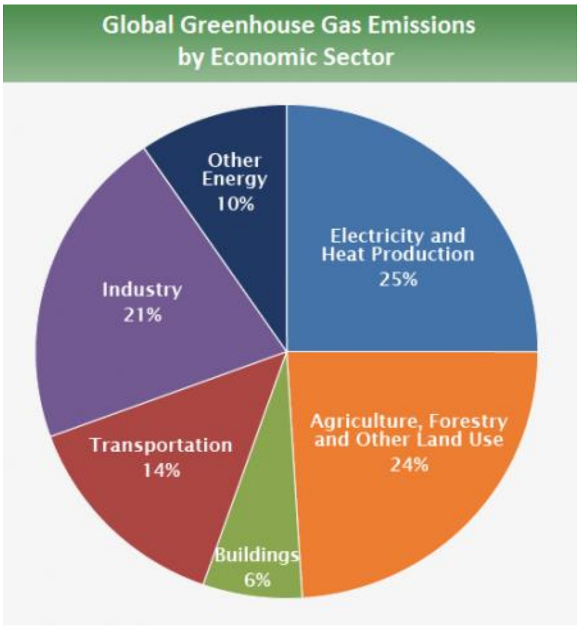

Appendix 7. The greenhouse gas emission by source sector in EU

(Source: EEA. 2017)

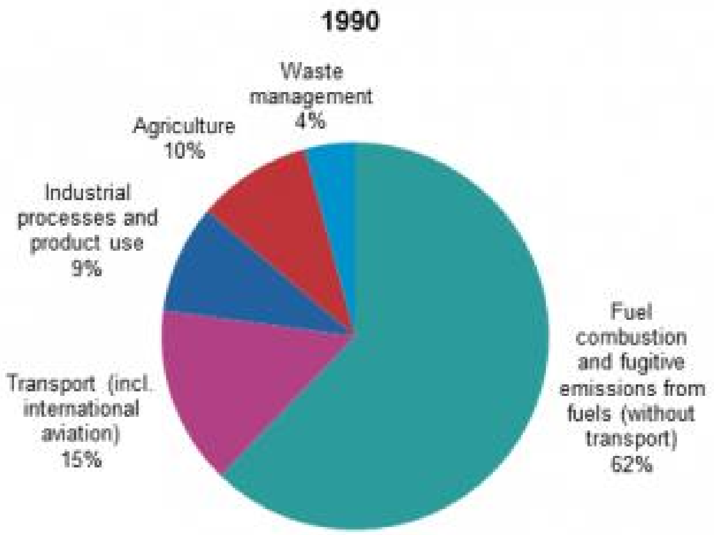

Appendix 8. Data comparison among EPA, EDGAR, and FAO on GHGs emission from agriculture sector

(Source: IPCC, AR5)

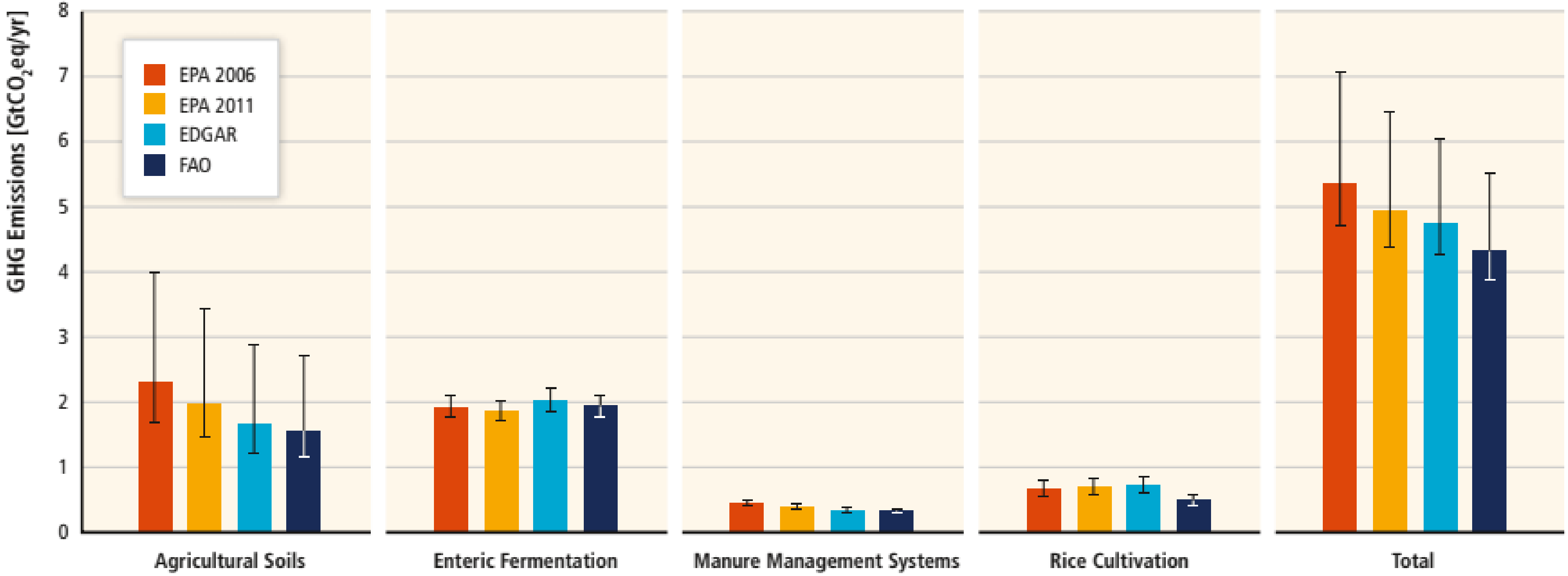

Appendix 9. GHGs emission from the agriculture sector in different regions in comparison to several data sources

(Source: FAOSTAT, 2013; EDGAR (JRC/PBL, 2013); U.S. EPA, 2013; (IPCC, AR5))

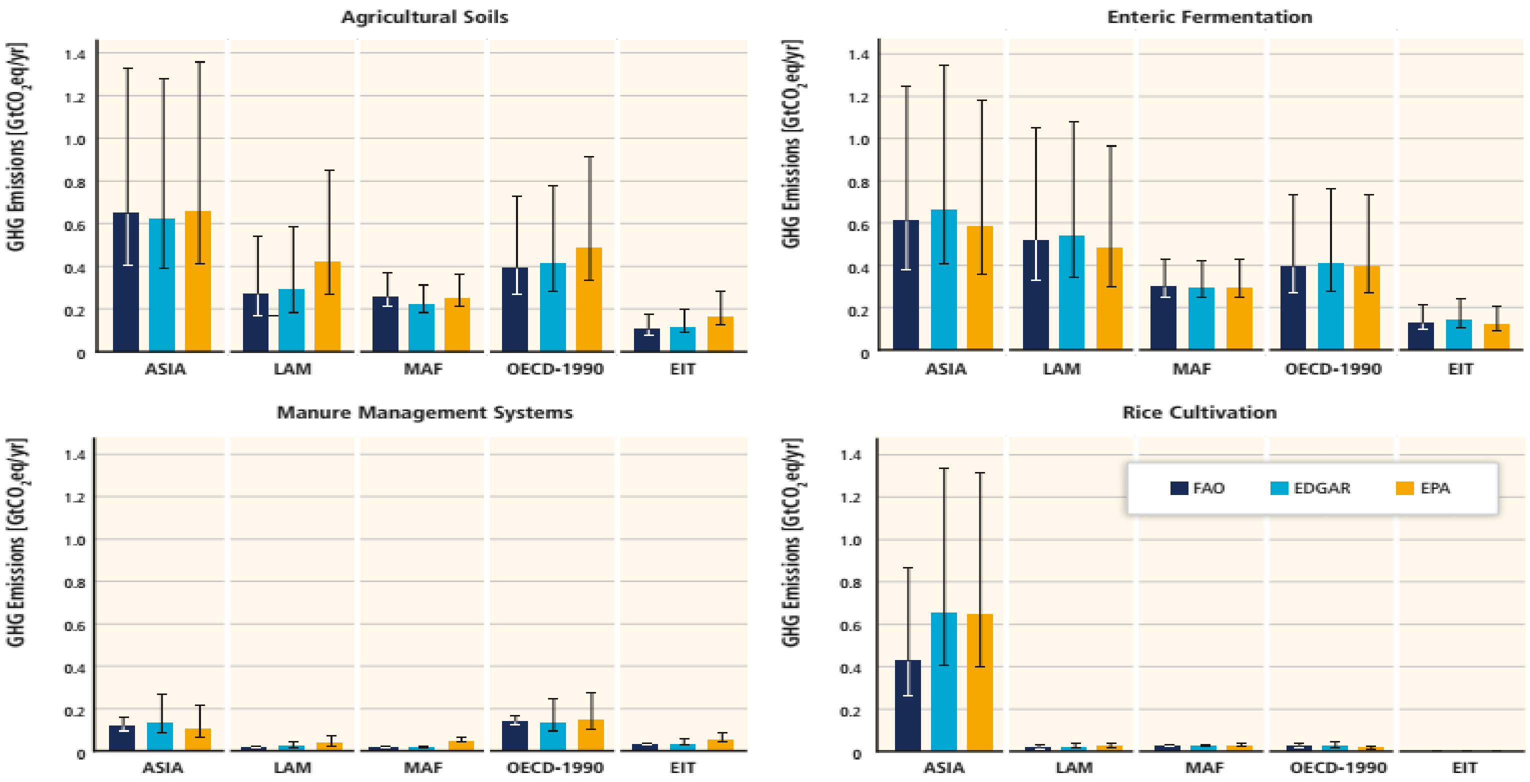

Appendix 10. The GHGs emission in EU-28, 2012 (Eurostat. 2016)

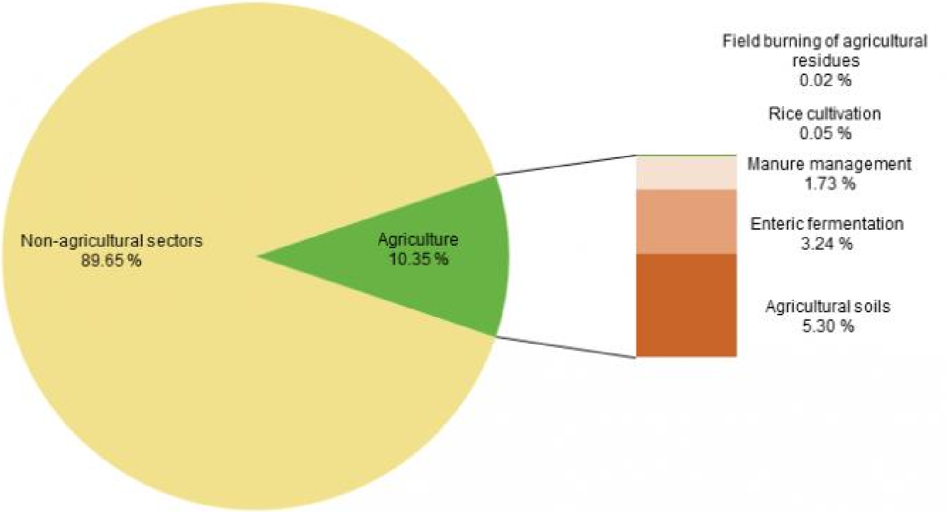

(*) Land use, land use change and Forestry (LULUCF) net removals are not included in total greenhouse gas emissions. Emissions from agricultural transport and energy use are not included in agriculture emissions, as these sectors are not defined as part of the agriculture sector by the current IPCC reporting guidelines.

Appendix 11. Table of carbon loss and its influencing factors at sites

Site	**decomposition**	**pH.CaCl2.**	**CN.median**	**drain**	**T_degC_median**	**gwh_m_median**	**Hrtop**	**Hwtop**	**C.kg_m2_sem**	**C.kg_m2**	**CLoss.kg_m2_sem**	**CLoss.kg_m2**
DK01	10	5.69	11.71	1	8.5	-0.11	-0.57	-0.45	6.994499052	84.68337615	5.193491025	18.13633906
DK02	10	6.14	12.38	1	9.01	-0.66	-0.7	-0.3	5.925715583	82.86904298	3.080861459	9.386867247
DK04	9	4.74	12.4	1	9.49	0.01	-0.3	0	2.445076523	53.13375619	0.818080148	16.90255245
DK05	10	4.35	12.47	1	8.97	-0.04	-0.4	-0.3	1.790917689	76.36698295	1.582863042	3.030512251
DO01	10	5.73	11.27	1	10.04	-0.56	-0.8	-0.5	6.946969556	106.4043714	3.162079387	6.323862152
DO03	9	5.81	10.85	1	9.86	-0.11	NA	-0.25	1.255859739	56.99228506	1.372165693	15.3989121
EE01	NA	2.88	52.3	1	6.21	-0.71	-0.4	-0.1	4.326859416	76.78745079	0	0
EE04	10	6.25	13.64	1	7.33	-0.54	-2.7	-0.6	3.719976522	109.4997139	9.955035719	68.20915216
EE05	10	6.25	13.88	1	7.77	-0.8	-0.72	-0.42	1.530473643	108.575963	1.138830255	33.6380326
EE06	10	6.41	14.58	1	6.97	-0.38	-0.64	-0.39	5.925017272	107.7480786	4.527877794	28.25240155
EE07	10	7.12	12.87	1	6.93	-0.34	NA	-0.5	1.243961436	127.7820514	0	0
NLS01	10	5.44	11.49	2	11	-0.36	-0.6	-0.4	1.829913878	111.7665999	4.688685464	85.91667532
NLS02	10	5.28	11.47	1	NA	-0.46	-0.6	-0.38	1.476005221	113.7056312	3.757584553	78.16548953
NLS03	10	4.92	10.78	2	13.04	-0.72	-0.55	-0.35	3.013848261	84.82698705	8.785121012	60.19597443
NLS04	10	4.64	10.74	1	11.12	-0.33	-0.55	-0.35	2.595676177	92.28673048	0.929225213	35.60857714
Site	**CPristine.kg_m2_sem**	**CPristine.kg_m2**	**S.m_sem**	**S.m**	**Sp.m_sem**	**Sp.m**	**Ss.m_sem**	**Ss.m**	**Analysed_Depth.m**	**Cultivation_time**	**Use_type**	
DK01	1.801008027	102.8197152	0.062337571	0.325961658	0.001097241	0.149086112	0.063434813	0.176875546	0.66	more than 100	rewetted	
DK02	2.844854124	92.25591023	0.033642655	0.130471832	0.000829457	0.042011065	0.034472112	0.088460767	0.72	more than 100	rewetted	
DK04	3.165893284	70.03630864	0.02178245	0.368069614	0.015285344	0.158159108	0.008024451	0.209910506	0.51	more than 100	egrass	
DK05	3.684032378	78.83553435	0.038362595	0.090316379	0.015698901	0.063285337	0.017752225	0.033300382	0.78	more than 100	egrass	
DO01	3.265258912	112.0060942	0.043885388	0.101108256	0.020805927	0.052866643	0.026718781	0.053163318	0.78	50-100	igrass	
DO03	1.374705502	72.39119716	0.01339423	0.259139334	0.01498548	0.058021045	0.017291454	0.201118289	0.69	more than 100	pasture	
EE01	4.869642499	75.05585371	0	0	1.84E-17	3.47E-17	0	0	0.96	0	extraction	
EE04	12.29253463	177.7088661	0.061978274	0.643696927	0.019341795	0.060597715	0.06984444	0.583099212	0.9	52	igrass	
EE05	0.494067239	142.2139956	0.00612384	0.409722549	0.007186151	0.087871382	0.013286832	0.321851167	0.96	52	wheat	
EE06	6.977710123	136.0004802	0.037636821	0.538505415	0.00736919	0.273421642	0.04352189	0.265083772	0.75	41	igrass	
EE07	1.500366108	125.8815678	0	0	1.31E-17	2.43E-17	0	0	0.87	41	barley	
NLS01	4.830814522	197.6832753	0.058521484	1.0250305	0.007340926	0.229041177	0.051204952	0.795989323	0.87	50-100	igrass	
NLS02	2.467212746	191.8711207	0.032400739	0.960357007	0.007235798	0.213515566	0.039299408	0.746841441	0.93	50-100	igrass	
NLS03	6.101529638	145.0229615	0.078509879	0.795435082	0.025123768	0.196807779	0.092511857	0.598627303	0.72	50-100	igrass	
NLS04	3.003313492	127.8953076	0.025288244	0.586769281	0.01303655	0.22791999	0.013446544	0.358849291	0.78	50-100	igrass	

land cover types	sites	pristine carbon kg/m^2	carbon loss kg/m^2	carbon loss/pristine carbon
igrass	DO01	112	6.32	5.64%
	EE04	178	68.21	38.32%
	EE06	136	28.25	20.77%
	NLS01	198	85.92	43.39%
	NLS02	192	78.17	40.71%
	NLS03	145	60.2	41.52%
	NLS04	128	35.61	27.82%
wheat	EE05	142	33.64	23.69%
pasture	DO03	72	15.4	21.39%
egrass	DK04	70	16.9	24.14%
	DK05	79	3.03	3.84%
rewetted peatland	DK01	103	18.14	17.61%
	DK02	92	9.39	10.21%
extracted peatland	EE01	75	0	0.00%
barley	EE07	126	0	0.00%

land cover type	pristine carbon.$_{median}$ kg/m^2	carbon loss.$_{median}$ kg/m^2	carbon loss.median /pristine carbon.median
igrass	145	60.2	41.52%
wheat	142	33.64	23.69%
pasture	72	15.4	21.39%
rewetted peatland	98	13.765	14.12%
egrass	75	9.965	13.38%
extracted peatland	75	0	0.00%
barley	126	0	0.00%

land cover type	pristine carbon.$_{median}$ kg/m^2	carbon loss.$_{median}$ kg/m^2	carbon loss.median /pristine carbon.median
grass land	132	31.93	24.19%
arable land	142	33.64	23.69%

* grassland refers to intensively managed grassland, pasture and extensively managed grass land; arable land refers to wheat

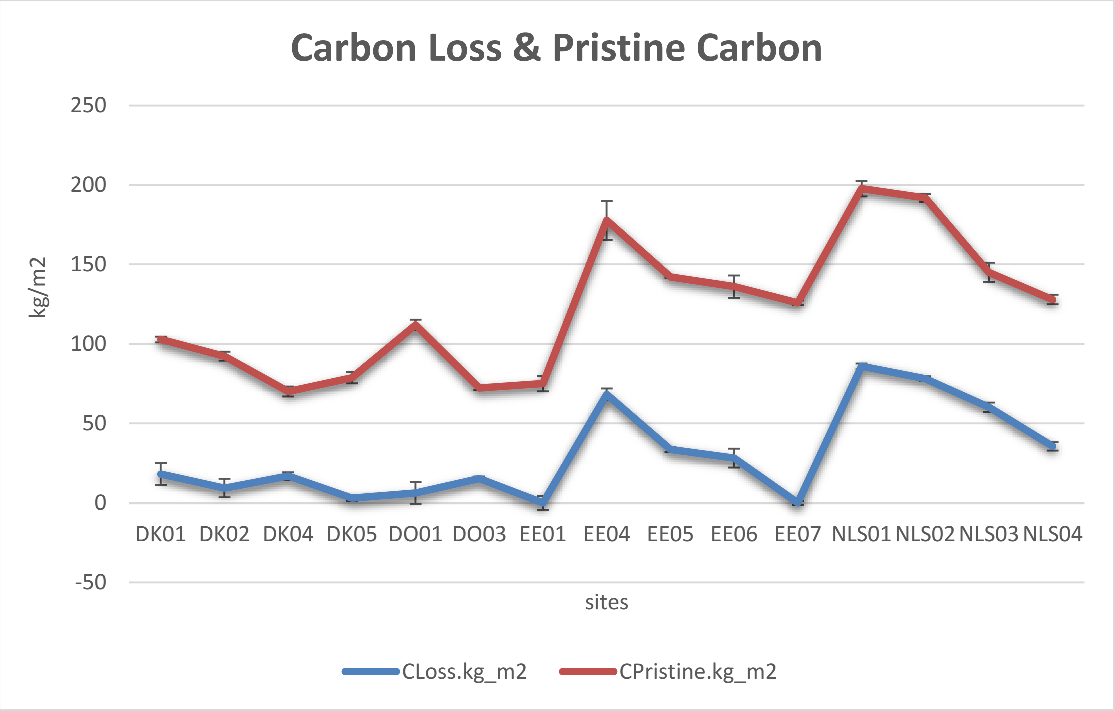Appendix 13. A comparison of carbon loss and pristine carbon at sites